Sphingosine-1-phosphate Prevents Egress of Hematopoietic Stem Cells From Liver to Reduce Fibrosis

Accepted Manuscript

Sphingosine-1-phosphate Prevents Egress of Hematopoietic Stem Cells From Liver to Reduce Fibrosis

Andrew King, Diarmaid D. Houlihan, Dean Kavanagh, Debashis Haldar, Nguyet Luu, Andrew Owen, Shankar Suresh, Nwe Ni Than, Gary Reynolds, Jasmine Penny, Henry Sumption, Prakash Ramachandran, Neil C. Henderson, Neena Kalia, Jon Frampton, David H. Adams, Philip N. Newsome

PII: S0016-5085(17)30331-1
DOI: 10.1053/j.gastro.2017.03.022
Reference: YGAST 61054

To appear in: *Gastroenterology*
Accepted Date: 18 March 2017

Please cite this article as: King A, Houlihan DD, Kavanagh D, Haldar D, Luu N, Owen A, Suresh S, Than NN, Reynolds G, Penny J, Sumption H, Ramachandran P, Henderson NC, Kalia N, Frampton J, Adams DH, Newsome PN, Sphingosine-1-phosphate Prevents Egress of Hematopoietic Stem Cells From Liver to Reduce Fibrosis, *Gastroenterology* (2017), doi: 10.1053/j.gastro.2017.03.022.

Title: Sphingosine-1-phosphate Prevents Egress of Hematopoietic Stem Cells From Liver to Reduce Fibrosis

Short title: Hematopoietic stem cells reduce liver fibrosis

Andrew King*[1], Diarmaid D Houlihan[1], Dean Kavanagh[2], Debashis Haldar[1], Nguyet Luu[1], Andrew Owen[1], Shankar Suresh[1], Nwe Ni Than[1], Gary Reynolds[1], Jasmine Penny[1], Henry Sumption[1], Prakash Ramachandran[3], Neil C Henderson[3], Neena Kalia[2], Jon Frampton[4], David H Adams[1], Philip N Newsome*[1].

[1]National Institute for Health Research (NIHR) Birmingham Liver Biomedical Research Unit and Centre for Liver Research, University of Birmingham, Birmingham, UK.

[2]Centre for Cardiovascular Sciences, College of Medical and Dental Sciences, University of Birmingham.

[3]MRC Centre for Inflammation Research, University of Edinburgh, Edinburgh, United Kingdom

[4]School Institute of Immunology and Immunotherapy, College of Medical and Dental Sciences, University of Birmingham.

Grant support: This work was funded by support from the Medical Research Council (Dr A King Clinical Training Fellowship). PNN is supported by the National Institute of Health Research (NIHR) Birmingham Liver Biomedical Research Unit (BRU). The views expressed are those of the authors and not necessarily those of the NHS, the NIHR or the Department of Health.

Abbreviations:

α-SMA, α-smooth muscle actin

CCl_4, carbon tetrachloride

CLP, common lymphoid progenitors

CMP, common myeloid progenitors

DiR, 1,1'-Dioctadecyl-3,3,3',3'-Tetramethylindotricarbocyanine Iodide

ECM, extracellular matrix

HPC7, hematopoietic progenitor cell line

HSC, hematopoietic stem cell

IVIS, In Vivo Imaging System

MCD, Methionine choline deficient

MMP, Matrix metalloproteinase

NL, normal liver

PSR, picrosirius red

S1P, Sphingosine 1-phosphate

SphK1, Sphingosine kinase 1

SGPP1, Sphingosine-1-phosphate phosphatase

SGPL1, Sphingosine-1-phosphate lyase

* Corresponding Authors

Professor Philip Newsome

NIHR Birmingham Liver Biomedical Research Unit and Centre for Liver Research

5th Floor Institute of Biomedical Research

University of Birmingham

Birmingham

B15 2TT

UK

Telephone: +44-121-415-8700

Fax: +44-121-415-8701

Email: P.N.Newsome@bham.ac.uk

Dr Andrew King

NIHR Birmingham Liver Biomedical Research Unit and Centre for Liver Research

5th Floor Institute of Biomedical Research

University of Birmingham

Birmingham

B15 2TT

UK

Telephone: +44-121-415-8700

Fax: +44-121-415-8701

Email: andyking@doctors.org.uk

Disclosures: No relevant disclosures.

Author contributions: AK and PNN with JF and DHA had the original concept and contributed to the design of the study protocol. NH & PR provided intellectual contribution to the study. AK, with the assistance of DDH, DK, DH, NL, AO, SS, NNT, GR, JP, NK and HS performed the experiments and generated all of the data for the manuscript. AK performed the statistical analysis. PNN and AK wrote the first draft of the manuscript, and all authors reviewed the final version. PNN is guarantor.

Abstract

Background & Aims: There is growing interest in the use of bone marrow cells to treat liver fibrosis, however little is known about their anti-fibrotic efficacy or the identity of their effector cell(s). Sphingosine-1-phosphate (S1P) mediates egress of immune cells from the lymphoid organs into the lymphatic vessels; we investigated its role in the response of hematopoietic stem cells (HSC) to liver fibrosis in mice.

Methods: Purified (c-kit+/sca1+/lin-) hematopoietic stem cells (HSC) were repeatedly infused into mice undergoing fibrotic liver injury. Chronic liver injury was induced in BoyJ mice by injection of carbon tetrachloride (CCl4) or placement on methionine/choline deficient (MCD) diets. Some mice were irradiated and given transplants of bone marrow cells from C57BL6 mice, with or without the S1P antagonist FTY720; we then studied HSC mobilization and localization. Migration of HSC cell lines was quantified in trans-well assays. Levels of S1P in liver, bone marrow and lymph fluid were measured using an ELISA. Liver tissues were collected and analyzed by immunohistochemical, quantitative PCR and sphingosine kinase activity assays. We performed quantitative PCR analyses of expression of sphingosine kinase 1 and 2 (SphK), sphingosine-1-phosphate lyase 1 (SGPL1), and sphingosine-1-phosphate phosphatase 1 (SGPP1) in normal human liver and cirrhotic liver from patients with alcohol related liver disease (n=6).

Results: Infusions of HSC into mice with liver injury reduced liver scarring based on picrosirius red staining (49.7% reduction in mice given HSC vs control mice; P<.001), and hepatic hydroxyproline content (328 mg/g in mice given HSC vs 428 mg/g in control mice; *P*<.01). HSC infusion also reduced hepatic expression of alpha smooth muscle actin (0.19±0.007-fold compared with controls; *P*<.0001) and collagen type I alpha 1 chain (0.29±0.17-fold compared with controls; *P*<.0001). These anti-fibrotic effects were maintained with infusion of lymphoid progenitors that lack myeloid potential and associated with increased numbers of recipient neutrophils and macrophages in liver. In studies of HSC cell lines, we found HSC to recruit monocytes, and this process to require C-C motif

chemokine receptor 2. In fibrotic liver tissue from mice and patients hepatic S1P levels increased due to elevated hepatic sphingosine kinase-1 expression, that contributed to a reduced liver:lymph S1P gradient and limited HSC egress from the liver. Mice given the S1P antagonist (FTY720) with HSC had increased hepatic retention of HSC (1697±247 cells in mice given FTY720 vs 982±110 cells in controls; *P*<.05) and further reductions in fibrosis.

Conclusions: In studies of mice with chronic liver injury, we demonstrated the anti-fibrotic effects of repeated infusions of purified HSC. We found that HSC promote recruitment of endogenous macrophages and neutrophils. Strategies to reduce SIP signaling and increase retention of HSC in the liver could increase their anti-fibrotic activities and developed for treatment of patients with liver fibrosis.

KEY WORDS: mouse model, CCR2, sphingolipid, immune cell localization

Background and Aims

The incidence of chronic liver disease is rising worldwide[1] and is characterised by the progression of liver injury from hepatic fibrosis to cirrhosis, resulting in death from liver failure, complications of portal hypertension or hepatocellular carcinoma[2]. At present liver transplantation remains the only curative treatment for end stage liver disease but is limited by availability of donor organs and the risks of lifelong immunosuppression[3-5]. The development and resolution of hepatic fibrosis is recognised as a bidirectional process, with resolution of fibrosis mediated through degradation of hepatic collagen[6] and apoptosis of activated hepatic myofibroblasts[7].

Initial observations that bone marrow cells may contribute to hepatic repair and regeneration[8-10] were followed by studies in animal models of chronic liver injury demonstrating variable therapeutic effects[11-14]. Despite these mixed outcomes multiple clinical studies of BM-derived stem cell therapy have already been performed[15-17]. The design of these studies has not permitted any meaningful conclusions and larger randomised controlled trials are underway.

The heterogeneous nature of the bone marrow cell populations studied to date has limited our understanding of their beneficial effects and prevented elucidation of potential mechanisms. Hematopoietic stem cells (HSC) reside with the bone marrow niche, provide continual renewal and replacement of all blood cell lineages[18] and can be routinely isolated using cell surface markers[19]. The continual homeostatic recirculation of bone marrow stem cells has recently been described and the bioactive sphingolipid Sphingosine 1-phosphate (S1P) identified as a key regulator of this process[20]. An S1P concentration gradient between body compartments is established by varying tissue distribution of sphingosine kinase (SPHK1/2) and sphingosine-1-phosphate lyase (SGPL)/ sphingosine-1-phosphate phosphatase (SGPP)[21, 22] and this gradient regulates the egress of HSC from peripheral tissue into draining lymphatics. Binding of FTY720, a functional antagonist , to S1P receptors results in internalisation and ubiquitin-dependent degradation without downstream

signalling, thus rendering cells unresponsive to S1P[23]. This blocks egress of HSC resulting in an accumulation of HSC within peripheral tissues[20].

We studied the effect of chronic liver injury on HSC mobilisation and recruitment to the liver and demonstrated reduced hepatic fibrosis after repeated therapeutic administration of a purified population of HSC. Furthermore, we observed changes in S1P expression in chronic liver injury and demonstrated prolonged hepatic retention of HSC after administration of FTY720 which resulted in a further significant reduction in liver fibrosis when administered in conjunction with KSL cell injections.

Methods

Murine Models of Liver Injury

Mice were housed in a temperature controlled sterile animal facility with 12 hour light/dark cycles and free access to food and water. All experiments were conducted in accordance with the University of Birmingham ethics policy and the UK Animals (Scientific Procedures) Act 1986 (Project Licence PPL 40/3201). C57/BL6 mice were obtained from Charles River Laboratories and BoyJ mice from a colony maintained at the Biomedical Services Unit of the University of Birmingham. To induce chronic liver injury carbon tetrachloride (CCl_4, Sigma, 1mg/kg diluted 1:4 in mineral oil) was injected twice weekly for 9 weeks, with control mice receiving mineral oil vehicle only. In separate experiments mice were fed either standard chow or a methionine choline deficient (MCD) diet (MP Biomedical) for 6 weeks.

Experimental Protocols

6-8 week old female BoyJ mice received twice weekly intraperitoneal injection of CCl_4 (1mg/kg in mineral oil) for 6 weeks then randomly allocated to receive either purified cells isolated from 6-8 week old male C57BL6 mice as described, or no treatment. Cell injections were administered on the first day of weeks 7,8 and 9 of liver injury and mice were sacrificed one week following the final cell injection and 72 hours after the final CCl_4 injection. In some experiments FTY720 (Cayman Chemicals, 1mg/kg in PBS + 0.1 % DMSO) or vehicle control was administered by intraperitoneal injection three times per week from week 6 until sacrifice.

Bone Marrow Transplantation

6 week old C57/BL6 mice received lethal irradiation (9Gy in 2 divided doses) followed by transplantation via tail vein injection of $1x10^8$ whole bone marrow cells isolated from 6 week old BoyJ mice. After four weeks, mice were randomly allocated to receive either twice weekly injection of CCl_4 (1 mg/kg) or mineral oil vehicle, for eight weeks followed by sacrifice.

Immunohistochemistry

Picrosirius red staining was performed using 0.1% Direct Red 80 (Sigma) in saturated picric acid according to standard protocols. Quantification of Picrosirius red and αSMA staining was performed by threshold analysis of 10 non overlapping randomly selected fields of view per slide at x20 magnification using ImageJ software (NIH) and expressed as % positive staining of total area. F4/80 and Ly6G staining was quantified by counting individual positive cells in 6 non overlapping randomly selected fields of view per slide at x20 and x100 magnification and expressed as cells per field of view.

S1P and SphK Quantification

SphK activity was determined using the Sphingosine Kinase Activity Assay (K-3500, Echelon) according to the manufacturer's instructions, a standard curve was created and results normalised to protein content of the sample and time (pmol S1P/mg protein/min). S1P concentrations were measured using the Sphingosine 1-phosphate ELISA kit (K-1900, Echelon) according to the manufacturer's instructions, S1P concentrations in serum and lymph fluid were expressed as molar quantities and in liver and bone marrow were normalised to the protein content of the sample (pmol S1P / mg protein).

Chemotaxis Assay

600µl Stem Pro 34 serum free media alone or containing the relevant concentration of S1P (Cayman chemicals) was placed in individual wells of a 12 well plate (Corning) and 6.5mm transwell inserts (5µm pore diameter) placed in each well. 100µl of cell suspension ($1x10^6$ cells/ml) was added to the insert and incubated for 3 hours. Cell migration was assessed by quantification of the number of cells in each lower using flow cytometry as described; migration was expressed as a percentage of the input cells in the lower well. S1P and FTY702-P were prepared by dissolving in 95%DMSO/5% 1N

HCl (Sigma) and diluted for use in PBS + 3% fatty acid free BSA (Sigma). W146 (Sigma) was dissolved in methanol containing 0.05% acetic acid and dilute for use in cell culture media.

Cell Culture

Studies of HSC trafficking have been limited by difficulties in isolating sufficient number of cells, in some experiments in this study we utilised an immortalised HSC line (HPC-7) which express common murine HSC markers and transcription factors[24], and have been used in previous studies of HSC recruitment[25]. HPC-7 cells were cultured in StemPro Serum Free Media 34 (Invitrogen) supplemented with penicillin, streptomycin, glutamine and 100ng/ml recombinant murine Stem Cell Factor (Invitrogen). For colony forming unit assays cells were added to Methocult GF media(Stem Cell Technologies) and incubated for 10 days, total number of myeloid colonies per assay were determined by counting under low power magnification.

Statistics

Statistical analyses were performed using GraphPad Prism version 5.0. Differences between groups were analysed using either the two tailed unpaired student's t-test or multiple group comparisons with one way ANOVA with Bonferroni post-test correction unless otherwise stated. A result was considered significant when $p<0.05$.

Results

Bone marrow derived HSC are mobilised and recruited to the liver during chronic liver injury

The effect of liver injury on the mobilisation and recruitment of BM-derived HSC was investigated in the model of carbon tetrachloride (CCl_4) induced liver injury. Higher numbers of HSC (termed KSL; c-kit$^+$, sca-1$^+$ and lineage^{neg}), were isolated from the peripheral blood (0.397±0.05 vs 0.065±0.07 KSL cells/µl blood, p<0.001) and liver (1163±173 vs 258.5±22 KSL cells/liver, p<0.01) of mice with CCl_4 injury compared with control mice (Figure 1B). There were also marked increases in colony forming unit potential from cells isolated from liver and peripheral blood, but not BM, in CCl_4 injury (Figure 1C). Similar results were seen in the setting of methionine choline deficient (MCD) diet induced liver injury. Liver resident populations of HSC have been described (Taniguchi et al 1996) and further studies to confirm the bone marrow origin of the isolated KSL cells were performed. Bone marrow chimerism was established (Supplementary Figure 1) and donor BM-derived HSC were identified as CD45.2$^+$ KSL. Significant increases in CD45.2$^+$ KSL cells were observed within the liver (788.2±59 vs 292.6±45, p<0.01) and peripheral blood (0.333±0.06 vs 0.077±0.01, p<0.01) of CCl_4-injured mice (Figure 1D), whilst BM populations remained constant. Given the mobilisation and hepatic recruitment of HSC in liver injury the potential therapeutic benefits of administering purified HSC was investigated.

Infused KSL cells reduce fibrosis in the CCl_4 model of liver injury

KSL HSC were isolated from donor bone marrow and purity of >96% confirmed in all experiments (Supplementary Figure 2). Repeated injections of KSL cells (Figure 2A) resulted in a 49.7% reduction in hepatic fibrosis determined by Picrosirius red (PSR) quantification (2.21±0.12 vs 4.38±0.27 % staining, p<0.0001)(Figure 2B), and by reduced hepatic hydroxyproline content (328.5±30.4 vs 428.4±31.9 µg/g liver, p<0.05) (Figure 2C). Resolution of fibrosis is dependent upon apoptosis of

alpha smooth muscle actin (αSMA^+) myofibroblasts within the liver, and αSMA staining was 65.6% lower following KSL cell injections (2.42±0.2 vs 7.05±0.33, p<0.0001)(Figure 2D) and associated with downregulation of hepatic αSMA (0.19±0.007 fold vs control, p<0.0001) and col1a1 (0.29±0.17 fold vs control, p<0.0001) gene expression (Figure 2E). Serum albumin was higher in treated mice than untreated controls (4.06±0.37 vs 3.14±0.39, p<0.01)(Figure 2F). There were also increases in hepatic oval cell numbers (Figure 2G).

Anti-fibrotic effect of KSL cells is associated with enhancement of endogenous repair mechanisms

The fate of injected cells was investigated, but donor derived $CD45.2^+$ cells could not be detected in significant numbers within the liver 7 days after injection. Quantification of cell populations within the liver revealed a 219% increase in neutrophils (12.4±2.7 vs 5.646±2.51 $Ly6G^+$ cells per fov, p<0.0001) and a 177% in macrophages (44.2±11.8 vs 24.99±7.5 $F4/80^+$ cells per fov, p<0.0001) following KSL injections (Figure 3A/B). The absence of CD45.2 staining indicated that these increases were due to rises in endogenous cell populations rather than differentiation of injected KSL. Whilst, there were increases in MMP9 and 13 expressing cells (Figure 3C), and a reduction in the Arg-1/iNos ratio (Figure 3C), in the livers of mice receiving KSL infusions, there were no differences in macrophage sub-sets within the liver (Figure 3E) or blood (Supplementary Figure 3A-C), after KSL cell infusion. Ratio of $Ly\text{-}6C^{hi}$/$Ly\text{-}6C^{lo}$ (M1-like to M2-like) macrophages was not different between control (0.23) and KSL groups (0.12). Murine monocytes migrated towards HPC-7 cells in a dose-dependent fashion and at similar levels to CCL2 (Figure 3F), a classical monocyte chemoattractant. This migration was chemokine dependent as demonstrated by blockade seen after pertussis toxin (PTX) administration (Figure 3G). Notably the majority of this reduction was achieved when a CCR2-blocking antibody was used (Figure 3G).

Anti-fibrotic effect of KSL cells occurs irrespective of their myeloid differentiation potential

To explicitly establish whether anti-fibrotic effects of KSL were mediated through differentiation to macrophages, the effect of injecting committed myeloid or lymphoid progenitor cells was determined (Figure 4A). Common myeloid progenitors (CMP) established myeloid colonies whereas common lymphoid progenitors (CLP) did not (Figure 4B). Repeated injections of either progenitor population resulted in reduced hepatic fibrosis (Figures 4C/D), including a reduction in PSR staining (CMP 1.94±0.29, CLP 2.27±0.13, vs Control 4.38±0.27 % staining, $p<0.01$ both vs control)(Figure 4C) and a reduction in αSMA staining (CMP 2.79±0.25, CLP 3.69±0.33, vs control 7.05±0.39 % staining, $p<0.05$ both vs control)(Figure 4D). This anti-fibrotic effect was similar to that observed with injections of KSL and confirmed that myeloid differentiation was not required to mediate this effect. As with KSL cells, infusions of CMP and CLP cells were also associated with histological evidence of increased numbers of endogenous Ly6G neutrophils and F4/80 macrophages (Figure 4F/G) in the liver.

Hepatic sphingosine 1-phosphate expression and activity increases in rodent and clinical liver injury

As S1P, mediated by differences in concentration gradients, regulates the homeostatic trafficking of HSC between tissue compartments we determined changes in liver injury. In CCl_4 injury S1P levels were 1.7 fold higher in the liver (68.79±7.42 vs 39.45±7.06 pmol per mg protein, $p<0.05$) and 1.5 fold higher in the serum (1.71±0.13 vs 1.15±0.18 μM, $p<0.01$) with no significant change in BM or lymph concentrations (Figure 5A). To determine the factors influencing S1P levels we studied its cognate metabolising enzymes. SphK1 phosphorylates sphingosine to produce S1P and hepatic gene expression of SphK1 was upregulated during murine CCl_4 liver injury (5.57±0.65 fold vs control, $p<0.0001$) whilst expression of sphingosine kinase 2, SGPL and SGPP remained unchanged (Figure

5B). Similar findings were observed in human chronic liver disease (Figure 5C). SphK1 upregulation was not seen outside the murine liver (Supplementary Figure 4) and was also observed in mice fed the Methionine Choline deficient diet, an alternative model of chronic liver injury (Figure 5B). Analysis of isolated murine cell types demonstrated significant upregulation of SphK1 gene expression in liver sinusoidal endothelial cells during liver injury (5.26+/-1.26 fold vs control, $p<0.001$) without significant alteration in hepatocyte or PBMC gene expression (Figure 5D). SphK1 expression was 12 fold higher in human subjects with chronic liver disease than in normal controls (12.55±6.1 fold vs control, $p<0.01$)(Figure 5C) and this observation held true for different aetiologies of liver disease (Supplementary figure 5). SphK1 was the most abundant enzyme in hepatic sinusoidal endothelial cells and peripheral blood mononuclear cells, whereas hepatocytes predominantly expressed SGPL and SGPP (Figure 5E). Increased SphK1 was detected by Western blotting (Figure 5F) in both murine and human chronic liver injury and SphK1 enzymatic activity was 2.7 fold higher (5.76±0.95 vs 2.07±0.25 nmol/min/mg protein, $p<0.01$)(Figure 5G) in liver tissue from mice with CCl_4 injury. SphK1 enzymatic activity was also increased in chronically diseased human liver tissue (Figure 5H).

Blocking migration to S1P with FTY720 specifically increases retention of KSL cells in the injured liver

S1P1 was the most highly expressed S1P receptor on KSL, which was predominantly found intracellularly (Supplementary Figure 8A/B). *In vitro* migration to S1P was dose-dependent and peaked at 1µM (Supplementary Figure 8C). The HPC-7 cell line had similar c-kit/sca-1 expression (with absence of lineage markers), comparable S1P/chemokine receptor expression (Supplementary Figure 7) and migrated to S1P *in vitro* (Supplementary Figure 6E). Treatment of KSL with FTY720 markedly impaired S1P dependent cell migration (Supplementary Figure 8D), as did treatment with the S1P1 specific antagonist W146. After administration of FTY720 to mice with CCl_4 injury higher

numbers of KSL were isolated from liver (1697±247 vs 982±110 KSL cells/liver, p<0.05) whilst the number of circulating KSL in peripheral blood was not altered (0.36±0.1 vs 0.43±0.14 KSL cells/μl)(Supplementary Figure 8E). DiR labelling of KSL did not affect their viability or proliferation and fluorescence intensity of labelled cells was maintained at 7days without transfer of dye to unlabelled cells (Supplementary Figure 9). DiR labelled HPC-7 cells were used to study the tissue distribution of injected HSC, which revealed rapid clearance from the lungs over the first 24-48 hours and ongoing accumulation within the liver over 48 hours followed by gradual clearance (Figure 6A-C). Only low levels of uptake were found in the spleen and kidneys. Administration of FTY720 did not alter initial localisation of injected cells in either the liver or lungs, however the numbers of HPC-7 remaining within the liver were 50% higher than control 4 days after injection and 86% at 7 days (Figure 6A-C). Based on these findings, tissue localisation of KSL cells was studied at a single time-point, 4 days after injection. Greater numbers of injected KSL cells were found within the liver in mice treated with FTY720 compared with untreated controls (13514±1506 vs 7687±1556 DiR labelled KSL cells/liver, p<0.05) (Figure 6D). Intravital microscopy studies demonstrated that treatment of KSL cells with FTY720 or W146 did not increase their recruitment to the injured liver (Control 10.3±0.6, FTY720 9.6±2.4, W146 9.0±1.15 cells/fov) 60 minutes after injection (Figure 6E/F).

Increased retention of KSL cells in the injured liver with FTY720 enhances their anti-fibrotic effect

Administration of FTY720 alone did not alter hepatic fibrosis or αSMA activation (Supplementary figure 10). Administration of FTY720 in conjunction with repeated KSL cell injections resulted in a further 16% reduction in PSR staining (1.86±0.10 vs 2.21±0.11 % staining, p<0.05)(Figure 7A/B) and a 12% reduction in hepatic hydroxyproline content (289.2±90.9 vs 328.9±83.6, p=0.05)(Figure 7C) compared to KSL cell injection alone. αSMA staining was 21% lower (1.82±0.19 vs 2.31±0.22, p<0.05)(Figure 7D) in the FTY + KSL group and hepatic gene expression of αSMA and Col1a1 remained suppressed in both groups (Figure 7E).

Conclusions

Despite the considerable interest in bone marrow cell therapy for liver disease there is still significant uncertainty regarding their efficacy. Moreover, there is also a lack of clarity as to which population of bone marrow cells is likely to be the most effective. In this manuscript we demonstrate that repeated injections of a purified population of murine hematopoietic stem cells result in a marked resolution of hepatic fibrosis, in association with an increase in hepatic populations of endogenous macrophages and neutrophils. In addition, we demonstrate that abrogation of the migration of hematopoietic stem cells down an S1P gradient results in their greater hepatic retention and a further reduction in liver fibrosis, thus establishing a new therapeutic paradigm for the use of hematopoietic stem cells in this setting.

It has previously been proposed that injected bone marrow cells differentiate into anti-fibrotic cells of a monocyte/macrophage lineage[11]. However we have demonstrated that myeloid differentiation is not required for cells to exert their anti-fibrotic effect in our study, as injection of lymphoid progenitor cells induced a similar amount of fibrosis resolution as injections of either myeloid progenitors or HSC. Neutrophils and macrophages, with expression of MMP 9 and MMP 13, are critical to the resolution of fibrosis[26, 27] and significant increases in these cell populations were observed in the livers of mice receiving cell injections. The experimental design of this study, utilising a CD45 mismatch, confirmed that these cells were recipient derived, representing activation of endogenous repair pathways rather than a direct anti-fibrotic action of the injected cells. These findings clarify that HSC exert a paracrine effect within the injured liver stimulating repair through recruitment of other cell populations, and indeed HSC have been shown to be potent secretory cells, mediating effector properties through cytokine stimulation of immune cell populations[28]. Further study of the chemokines and cytokines (eg CCL2, IL-10, TWEAK) secreted by HSC may provide further define the mechanisms involved. Notably, our data indicate that murine monocytes, which may

mediate the anti-fibrotic effect of HSC are recruited to CCL2 and also to murine HPC-7 cells in a CCR2-dependent manner suggesting that a potential mechanism by which monocytes are recruited/positioned within the injured liver relates to hematopoietic stem cell expressed/secreted chemokine ligands. There were no differences in the proportion of macrophage subsets within the liver, or as a ratio of Ly-6C^{hi}/Ly-6C^{lo} (M1-like to M2-like) macrophages, after KSL cell infusion. Similarly no differences were seen in peripheral blood analysis. As recognised by the literature, surface marker expression of macrophages is likely to be more complex and dynamic and thus even extensive panels do not completely characterise the full phenotype of macrophages *in vivo*[29]. The integral role of macrophages in mediating both the generation and resolution of fibrosis has been demonstrated by other groups including our previous work[30, 31].

It is assumed that homing of HSC to the injured liver is required for them to exert their anti-fibrotic actions although this has not been proven. Increased recruitment of hematopoietic stem cells to the liver has been reported in response to stress-induced signals, such as increased expression of Stromal Derived Factor-1, MMP-9, and Hepatocyte Growth Factor which recruit human CD34+ progenitors[32]. We have previously reported that the adhesion of human hematopoietic (CD34+) stem cells to human liver compartments is integrin and CD44 dependent and modulated by CXCR3 and CXCR4[33]. Our BM transplantation studies confirm that liver injury with CCl_4 increases the number of BM-derived HSC in the liver, but without any change in the number of HSC in other organs. There have been a variety of different approaches taken to the administration of stem cell therapy in both humans and animal models, the peripheral venous route represents the safest and most feasible mode of delivery and we have shown this to be effective, as cells injected into a peripheral vein exert a beneficial therapeutic effect. Analysis of the distribution of injected HSC demonstrated their accumulation within the lungs immediately after injection followed by a rapid clearance, whereas recruitment to the liver increased over the first 48 hours with a more gradual reduction in cell

numbers subsequently. Seven days after injection the number of injected HSC remaining within the liver was very small and explains the absence of detectable numbers of cells on tissue section analysis. The whole organ analysis in this study provided an accurate assessment of cell numbers, as previous studies have used tissue section analysis which may not accurately quantify small numbers of cells or provide appropriate comparisons between organs for example overestimating the number of injected cells within the lungs.

S1P has been recognised to mediate recirculation of HSC down S1P gradients from tissue back into lymph and the circulation[20], and we demonstrate that S1P levels and activity are increased in the injured liver, thus partially reversing the normal S1P liver tissue:lymph gradient. Our data suggest that the increase in hepatic S1P levels is caused by upregulation of SphK1 in liver sinusoidal endothelial cells with less significant changes in other enzymes involved in S1P processing. To establish whether S1P was acting to increase recruitment of bone marrow-derived cells to the liver we performed intravital microscopy (Figure 6E/F) with blockade of the S1P axis using either a function-blocking antibody to S1P1 receptor or FTY720, neither of which altered the number of exogenously administered bone marrow-derived cells seen within the liver over a 60 minute period. We hypothesise therefore that the increased hepatic S1P levels act primarily to retain HSC within the liver by preventing their egress down the existing S1P liver-lymph gradient rather than priming the liver to recruit bone marrow-derived cells, which is in keeping with the observations of others in normal physiological conditions[20, 34].

To exploit this modulation of the S1P pathway we used pharmacological manipulation with the partial $S1P_1$ receptor agonist, FTY720. FTY720 impaired the migration of HSC *in vitro* and when administered to mice with liver injury resulted in accumulation of HSC within the liver. Whilst FTY720

did not affect trafficking of HSC within the first 48 hours after injection, increased numbers of injected HSC were present in mouse livers at later time-points compared with placebo controls. This supports our observations that HSC recruitment to the injured liver is not mediated through S1P receptors and that the increased number of HSC in the liver is a result of increased retention of HSC within the liver, rendered unresponsive to the S1P gradient by FTY720. The use of isolated KSL cells in these tracking studies was limited by the difficulties isolating the large number of cells required, and thus the findings from experiments using the HPC-7 cell line were used to design experiments with isolated KSL cells at a single time-point. This study, with KSL cells, also confirmed that mice receiving FTY720 had a greater number of cells within the liver four days after infusion.

Whilst administration of FTY could theoretically reduce homing to any organ our tracking data (Figure 6B-C) indicated no change in numbers of KSL cells found in the lungs. We believe therefore that the reason FTY720 increases the number of KSL cells in the liver, without an effect on other organs, is due to a combination of a reduced liver-lymphatic S1P gradient (due to the induction of liver injury which increases hepatic S1P levels) and a reduced tendency to migrate down an S1P axis due to the pharmacological action of FTY720. Notably, FTY720 has a range of systemic actions which in their own right may be anti-fibrotic, such as inhibiting of cytosolic phospholipase A2 and antagonising cannabinoid receptor 1[35], although in this study it had no anti-fibrotic effect when used in isolation. The anti-fibrotic effect of injected HSC was augmented by approximately 20% with the addition of FTY720 and although the clinical significance merits further study, any optimisation of the effect of this very rare population of cells should be considered advantageous. The optimal number of cells required to achieve an anti-fibrotic effect remains uncertain; in our studies we chose to administer lower numbers of cells than in previous studies and it is not clear whether the number of cells administered is proportional to the anti-fibrotic effect or whether there is a plateau effect beyond which no greater effect would be observed.

Our data demonstrate the potent anti-fibrotic actions of purified murine hematopoietic stem cells, and also indicate that enhanced exposure of the target organ, the injured liver, to infused HSC is associated with an augmentation of their anti-fibrotic effect. These findings support the development of clinical trials of stem cell therapy in humans.

Figure 1. Liver injury increases mobilisation and recruitment of HSC to the liver.

(A) c-kit$^+$ sca-1$^+$ lineage$^-$ (KSL) cells were quantified by flow cytometry and representative plots are shown. (B) Numbers of KSL cells were quantified in the peripheral blood, livers and bone marrow (BM) of CCl_4, MCD and mineral oil (MO) treated mice. Data from individual mice are displayed with means indicated by horizontal line (n=6 per group). (C) Colony forming potential of cells isolated from liver, blood and bone marrow were quantified in myeloid CFU assays. Data from individual mice are displayed with means indicated by horizontal line (n=6 per group). (D) BoyJ (CD45.1) mice were lethally irradiated (9Gy in 2 divided doses) and received unfractionated BM from C57Bl/6 (CD45.2) mice followed by administration of CCl_4 or MO for 8 weeks. Higher numbers of bone marrow derived CD45.2$^+$ KSL were found in the blood and livers of mice following CCl_4 liver injury (n=6 per group). * p<0.05, ** p<0.01, *** p<0.001.

Figure 2. Repeated injection of c-kit$^+$ sca-1$^+$ lin$^-$ hematopoietic stem cells (KSL) reduced hepatic fibrosis in a model of chronic carbon tetrachloride (CCl_4) liver injury.

(A) Liver injury was induced in eight week old C57/Bl6 mice by eight weeks of twice weekly intra-peritoneal injections of CCl_4. Mice were divided into two groups of 8 and one group received injections of $5x10^4$ KSL cells via tail vein at weeks six, seven and eight. Representative photomicrograph images of Picrosirius red staining (PSR) of livers demonstrate a reduction in collagen staining of livers from KSL treated mice, with loss of bridging fibrosis, compared to untreated control mice (magnification x40). Six random, non-overlapping images were obtained from each section and staining was quantified as a percentage of the image positive for PSR and αSMA using ImageJ software. Quantitative analysis of Picrosirius red staining (B) and biochemical measurement of hepatic hydroxyproline content (C) verified the reduction in hepatic fibrosis following KSL injections. The number of activated hepatic stellate cells, as indicated by

representative photomicrograph images of αSMA staining was reduced after KSL injections (D), which was confirmed by morphometric analysis of hepatic αSMA staining (D) and by hepatic gene expression of αSMA and col1a1 (E). Serum albumin levels were higher in mice receiving KSL injections (F). Hepatic oval cell numbers, as indicated by (G) Pan-CK were increased following KSL cell administration. Data are from n=8 per group and 3 independent experiments. * $p<0.05$, ** $p<0.01$, *** $p<0.001$ vs control.

Figure 3. Impact of administered hematopoietic stem cells (HSC) on endogenous cell recruitment and expansion in the injured liver.

There was a marked expansion in the number of recipient-derived Ly6G (A) and F4/80 (B) immuno-positive cells in the livers of mice after KSL injection as indicated in representative photomicrographs. (A) Ly6G and (B) F4/80 cells were counted manually in 6 random, non-overlapping fields of view (x100 F4/80, x20 Ly6G). (C) MMP9 and MMP13 expression in the liver was seen to increase following KSL cell administration, in association with a reduced Arg-1/iNOS expression ratio (D). Flow cytometric analysis of the digested livers (gating strategy in supplementary information) characterised the macrophage sub-sets within the liver (E). Murine monocytes were seen to trans-migrate towards CCL2 and HPC-7 HSC in a dose-dependent fashion (F). Migration of murine monocytes towards HPC-7 was chemokine dependent and inhibited by neutralising CCR2 antibody (G). Data are from n=8 per group and 3 independent experiments, expressed as mean +/- standard deviation of number of cells per field of view shown or median +/- IQR. * $p<0.05$, ** $p<0.01$.

Figure 4. Committed HSC sub-sets without myeloid properties are also able to reduce liver fibrosis.

(A) Representative plots of common myeloid progenitors and common lymphoid progenitors isolated using surface antigen expression (CMP: IL7Ra^{-} c-kit^{+} sca1^{+} lineage^{-}, CLP: IL7Ra^{+} c-kit^{lo} sca1^{lo} lineage^{-}). (B) KSL and CMP were able to form myeloid colonies *in vitro*, whereas CLP lacked this ability. Data are expressed as mean number of colonies per 500 plated cells shown (+/- SD) from three separate isolations. Tail vein injections of CMP or CLP cells at weeks 6,7,8 of CCl_4 injury, resulted in a similar reduction in hepatic fibrosis to that seen with KSL injections as assessed by quantitative analysis of picrosirius red staining, biochemical measurement of hepatic hydroxyproline content and hepatic gene expression for col1a1 (C). Similarly CMP and CLP injections also reduced the number of activated hepatic stellate cells to a level seen with KSL injections, as indicated by morphometric analysis of hepatic αSMA staining and by hepatic gene expression of αSMA (D). Serum albumin levels were also increased after CMP and CLP injections (E). There were increased numbers of endogenous Ly6G neutrophils (F) and F4/80 macrophages (G) in the liver after CMP and CLP infusions. Data are from n=8 per group and 3 independent experiments. * $p<0.05$ vs control.

Figure 5. Regulation of S1P levels in murine and human chronic liver injury.

(A) 8 week old C57/BL6 mice received CCl_4 or MO by i.p. injection twice weekly for 8 weeks. Sphingosine-1-phosphate (S1P) levels were higher in the livers and sera of mice following eight weeks of CCl_4 liver injury compared with MO controls, but were unchanged in bone marrow and lymph (n=5 per group). (B) Hepatic expression, by qPCR, of Sphingosine kinase 1 (SphK1) was increased, but there were no changes in gene expression for other enzymes (SphK2, SGPL1 & SGPP1) involved in S1P regulation (n=6 per group). A similar pattern of gene expression was observed mice fed an MCD diet, an alternative model of chronic liver injury (n=6 per group). (C) Hepatic gene expression of SphK1, SphK2, SGPL1 & SGPP1 were quantified in normal human liver and also human

cirrhotic liver from patients with alcohol related liver disease (n=6 per group). (D) Analysis of cell populations from chronically injured murine livers demonstrated upregulation of SphK1 gene expression in hepatic sinusoidal endothelial cells (LSEC), but not hepatocytes or peripheral blood mononuclear cells when compared with MO controls (n=3 per group, 3 independent experiments). Gene expression was also studied in constituent cells from explanted human cirrhotic livers and associated peripheral blood mononuclear cells (n=6 per group). (F) There was an increase in SphK1 protein expression in the CCl_4 treated mice by Western blotting (representative of 3 independent experiments). Samples of liver tissue were used in an ATP depletion assay to measure the enzymatic activity of SphK in injured and normal liver tissue (bottom left panel). The rate of phosphorylation of Sphingosine to S1P was higher in CCl_4 injured mice (G), as determined from the rate of depletion of ATP and expressed as nmol of S1P produced per minute per mg of liver protein (n=5 per group). Samples of human liver tissue were lysed for protein extraction and expression of SphK1 and GAPDH by Western blotting (representative of 3 independent experiments) demonstrated a rise in all cirrhotic liver samples (top right panel - F). The rate of phosphorylation of Sphingosine to S1P was higher in human chronic liver injury (H), as determined from the rate of depletion of ATP and expressed as nmol of S1P produced per minute per mg of liver protein (n=5 per group). * $p<0.05$, *** $p<0.001$ vs control..

Figure 6. FTY720 treatment increases the numbers of injected HSC within the liver.

DiR labelled HPC-7 cells were administered via tail vein to CCl_4 injured mice that were also treated with either FTY720 (1mg/kg) or vehicle control starting one day prior to cell injection and continuing for 7 days. (A) Representative combined photographic and fluorescence intensity images of livers from mice injected with HPC-7 cells treated with either FTY720 or vehicle at time points following cell injection. (B) The number of DiR labelled HPC-7 cells within the liver and lungs were then quantified using fluorescence intensity by (B) IVIS and (C) flow cytometric analysis of digested organs

up to 7 days after injection. Greater numbers of DiR labelled cells were detected in the liver at days 2, 4 and 7 after injection in mice treated with FTY720 (blue line) n=3 per group, 3 independent experiments). (D) Greater numbers of injected DiR-labelled KSL cells were present in the livers of mice treated with FTY720 (n=3 per group) using both fluorescence intensity by IVIS and by flow cytometric analysis of digested liver (n=3 per group, 3 independent experiments). (E) To establish if S1P has a role in engraftment of HSC to the liver (as well as retention) CFSE-labelled HPC-7 were pre-treated with FTY720, W146 or control media and injected into mice with CCl_4 liver injury. Recruitment of HSC to the liver was assessed in real time by intravital microscopy. Pre-treatment of HPC-7with FTY720 or W146 did not alter recruitment to injured liver for 60 minutes following injection (p=ns by two way ANOVA with Bonferroni multiple comparison test, n=3 per group, 6 independent experiments). (F) After completion of intra-vital microscopy experiments, liver tissue sections were analysed by fluorescent microscopy (FITC filter). The numbers of individual fluorescent cells were manually counted in 6 random, non-overlapping fields of view (x20 magnification) per section. No difference in numbers of injected cells within the liver was seen between cells treated with FTY720-P, W146 or control media (n=3 each group). * $p<0.05$, ** $p<0.01$.

Figure 7. FTY720 treatment augmented the anti-fibrotic effect of repeated HSC injection.

(A) Liver injury was induced in 8 week old C57/BL6 mice by eight weeks of twice weekly intra-peritoneal injections of CCl_4. Mice were divided into four groups; injury alone, injury and FTY720, injury and injection of $5x10^4$ KSL cells, or injury and injection of $5x10^4$ KSL cells and FTY720 (n=8-13 per group). Representative photomicrograph images of PSR staining of livers demonstrate a reduction in collagen staining of livers from KSL (+/- FTY720) treated mice, compared to control mice and those receiving FTY720 only (magnification x40). (B) Quantitative analysis of picrosirius red staining demonstrated that FTY720 treatment with KSL cell injections reduced hepatic fibrosis more than KSL injections alone (n=8-13 per group, 5 independent experiments), with a commensurate

reduction in level of (C) hepatic hydroxyproline (n=8-13 per group, 5 independent experiments). (D) Representative photomicrograph images of αSMA staining (magnification x40) across the four groups indicated lower levels of αSMA, as confirmed by morphometric analysis (n=13 per group, 5 independent experiments). (E) Hepatic gene expression of αSMA and col1a1 was supressed in both the KSL group and the KSL and FTY720 group (n=8-13 per group, 5 independent experiments). * $p<0.05$.

References

1. Leon DA, McCambridge J. Liver cirrhosis mortality rates in Britain from 1950 to 2002: an analysis of routine data. Lancet 2006;367:52-56.
2. D'Amico G, Garcia-Tsao G, Pagliaro L. Natural history and prognostic indicators of survival in cirrhosis: a systematic review of 118 studies. J Hepatol 2006;44:217-31.
3. Lucey MR, Terrault N, Ojo L, et al. Long-term management of the successful adult liver transplant: 2012 practice guideline by the American Association for the Study of Liver Diseases and the American Society of Transplantation. Liver Transpl 2013;19:3-26.
4. Merion RM, Schaubel DE, Dykstra DM, et al. The survival benefit of liver transplantation. Am J Transplant 2005;5:307-13.
5. NHSBT Liver Transplantation Activity Report (United Kingdom). 2012.
6. Iredale JP, Benyon RC, Pickering J, et al. Mechanisms of spontaneous resolution of rat liver fibrosis. Hepatic stellate cell apoptosis and reduced hepatic expression of metalloproteinase inhibitors. J Clin Invest 1998;102:538-49.
7. Kisseleva T, Cong M, Paik Y, et al. Myofibroblasts revert to an inactive phenotype during regression of liver fibrosis. Proc Natl Acad Sci U S A 2012;109:9448-53.
8. Petersen BE, Bowen WC, Patrene KD, et al. Bone marrow as a potential source of hepatic oval cells. Science 1999;284:1168-1170.
9. Theise ND, Badve S, Saxena R, et al. Derivation of hepatocytes from bone marrow cells in mice after radiation-induced myeloablation. Hepatology 2000;31:235-240.
10. Lagasse E, Connors H, Al-Dhalimy M, et al. Purified hematopoietic stem cells can differentiate into hepatocytes in vivo. Nat Med 2000;6:1229-34.
11. Sakaida I, Terai S, Yamamoto N, et al. Transplantation of bone marrow cells reduces CCl4-induced liver fibrosis in mice. Hepatology 2004;40:1304-1311.
12. Yannaki E, Athanasiou E, Xagorari A, et al. G-CSF-primed hematopoietic stem cells or G-CSF per se accelerate recovery and improve survival after liver injury, predominantly by promoting endogenous repair programs. Exp Hematol 2005;33:108-19.
13. Quintanilha LF, Mannheimer EG, Carvalho AB, et al. Bone marrow cell transplant does not prevent or reverse murine liver cirrhosis. Cell Transplant 2008;17:943-53.
14. Thomas JA, Pope C, Wojtacha D, et al. Macrophage therapy for murine liver fibrosis recruits host effector cells improving fibrosis, regeneration, and function. Hepatology 2011;53:2003-15.
15. Houlihan DD, Newsome PN. Critical review of clinical trials of bone marrow stem cells in liver disease. Gastroenterology 2008;135:438-50.
16. Moore JK, Stutchfield BM, Forbes SJ. Systematic review: the effects of autologous stem cell therapy for patients with liver disease. Aliment Pharmacol Ther 2014;39:673-85.
17. King A, Barton D, Beard HA, et al. REpeated AutoLogous Infusions of STem cells In Cirrhosis (REALISTIC): a multicentre, phase II, open-label, randomised controlled trial of repeated autologous infusions of granulocyte colony-stimulating factor (GCSF) mobilised CD133+ bone marrow stem cells in patients with cirrhosis. A study protocol for a randomised controlled trial. BMJ Open 2015;5:e007700.
18. Siminovitch L, McCulloch EA, Till JE. The Distribution of Colony-Forming Cells among Spleen Colonies. J Cell Physiol 1963;62:327-36.
19. Wognum AW, Eaves AC, Thomas TE. Identification and isolation of hematopoietic stem cells. Arch Med Res 2003;34:461-75.
20. Massberg S, Schaerli P, Knezevic-Maramica I, et al. Immunosurveillance by hematopoietic progenitor cells trafficking through blood, lymph, and peripheral tissues. Cell 2007;131:994-1008.
21. Pappu R, Schwab SR, Cornelissen I, et al. Promotion of lymphocyte egress into blood and lymph by distinct sources of sphingosine-1-phosphate. Science 2007;316:295-8.

22. Olivera A, Allende ML, Proia RL. Shaping the landscape: metabolic regulation of S1P gradients. Biochim Biophys Acta 2013;1831:193-202.
23. Oo ML, Thangada S, Wu MT, et al. Immunosuppressive and anti-angiogenic sphingosine 1-phosphate receptor-1 agonists induce ubiquitinylation and proteasomal degradation of the receptor. J Biol Chem 2007;282:9082-9.
24. Volpe G, Walton DS, Del Pozzo W, et al. C/EBPalpha and MYB regulate FLT3 expression in AML. Leukemia 2013;27:1487-96.
25. Kavanagh DP, Durant LE, Crosby HA, et al. Haematopoietic stem cell recruitment to injured murine liver sinusoids depends on (alpha)4(beta)1 integrin/VCAM-1 interactions. Gut 2010;59:79-87.
26. Harty MW, Papa EF, Huddleston HM, et al. Hepatic macrophages promote the neutrophil-dependent resolution of fibrosis in repairing cholestatic rat livers. Surgery 2008;143:667-78.
27. Fallowfield JA, Mizuno M, Kendall TJ, et al. Scar-associated macrophages are a major source of hepatic matrix metalloproteinase-13 and facilitate the resolution of murine hepatic fibrosis. J Immunol 2007;178:5288-95.
28. Granick JL, Simon SI, Borjesson DL. Hematopoietic stem and progenitor cells as effectors in innate immunity. Bone Marrow Res 2012;2012:165107.
29. Ju C, Tacke F. Hepatic macrophages in homeostasis and liver diseases: from pathogenesis to novel therapeutic strategies. Cell Mol Immunol 2016;13:316-27.
30. Duffield JS, Forbes SJ, Constandinou CM, et al. Selective depletion of macrophages reveals distinct, opposing roles during liver injury and repair. J.Clin.Invest 2005;115:56-65.
31. Ramachandran P, Pellicoro A, Vernon MA, et al. Differential Ly-6C expression identifies the recruited macrophage phenotype, which orchestrates the regression of murine liver fibrosis. Proc Natl Acad Sci U S A 2012;109:E3186-95.
32. Kollet O, Shivtiel S, Chen YQ, et al. HGF, SDF-1, and MMP-9 are involved in stress-induced human CD34+ stem cell recruitment to the liver. J.Clin.Invest 2003;112:160-169.
33. Crosby HA, Lalor PF, Ross E, et al. Adhesion of human haematopoietic (CD34+) stem cells to human liver compartments is integrin and CD44 dependent and modulated by CXCR3 and CXCR4. J Hepatol 2009;51:734-49.
34. Juarez JG, Harun N, Thien M, et al. Sphingosine-1-phosphate facilitates trafficking of hematopoietic stem cells and their mobilization by CXCR4 antagonists in mice. Blood 2012;119:707-16.
35. Paugh SW, Cassidy MP, He H, et al. Sphingosine and its analog, the immunosuppressant 2-amino-2-(2-[4-octylphenyl]ethyl)-1,3-propanediol, interact with the CB1 cannabinoid receptor. Mol Pharmacol 2006;70:41-50.

Figure 1

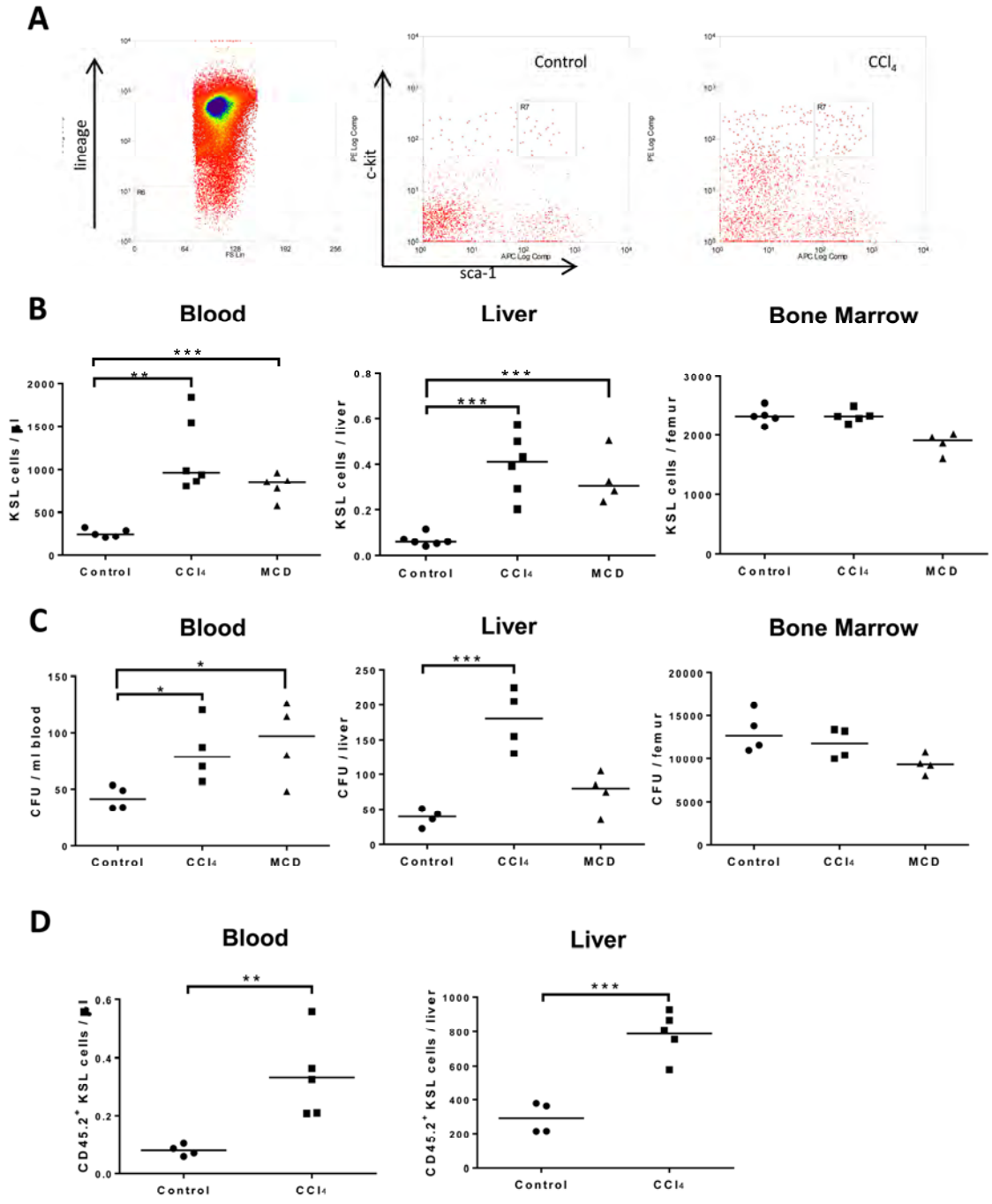
A
lineage
Control
CCl4
c-kit
sca-1
B
Blood
Liver
Bone Marrow
KSL cells / ml
KSL cells / liver
KSL cells / femur
Control
CCl4
MCD
C
Blood
Liver
Bone Marrow
CFU / ml blood
CFU / liver
CFU / femur
D
Blood
Liver
CD45.2+ KSL cells / ml
CD45.2+ KSL cells / liver

Figure 2

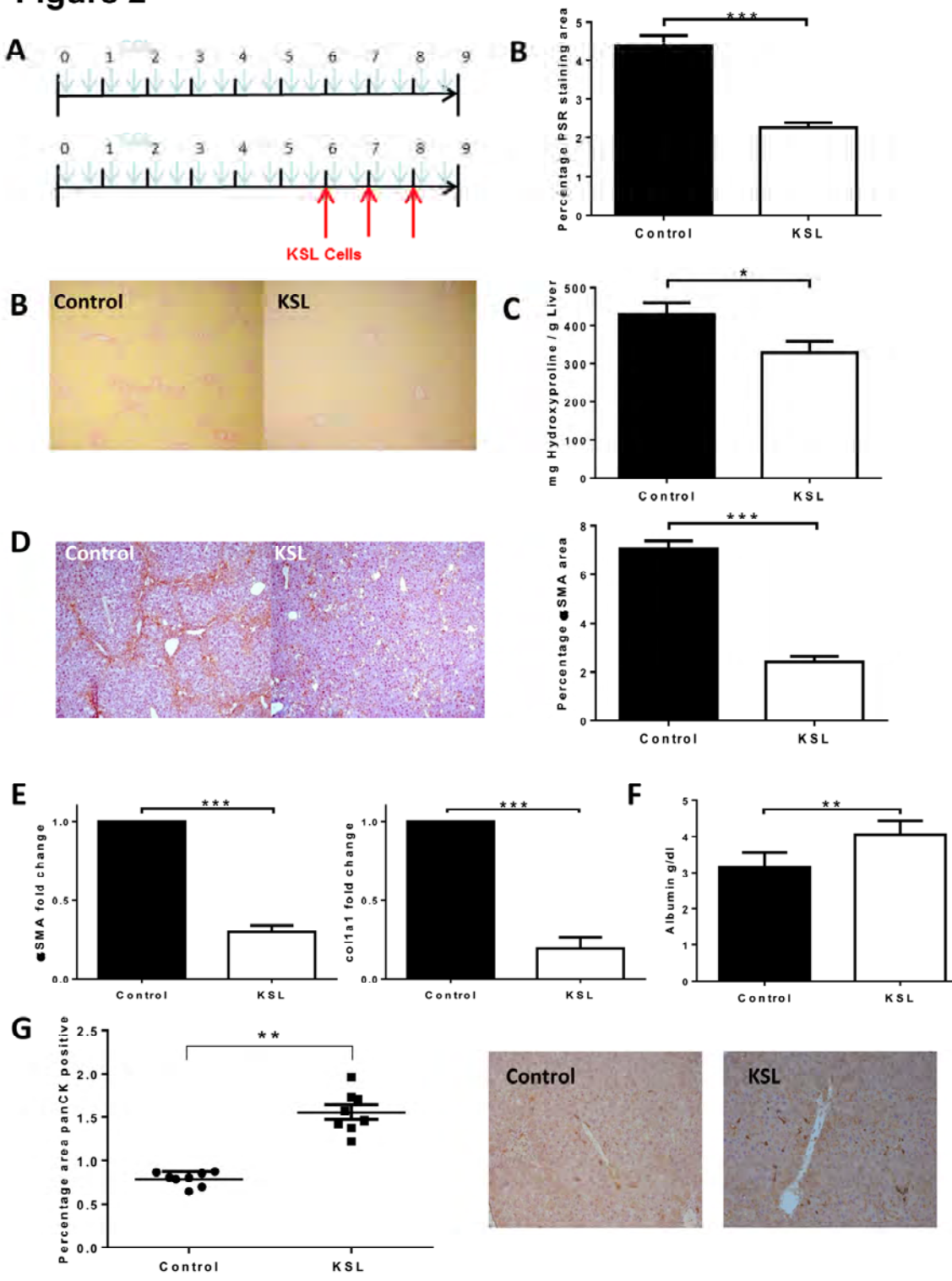
A
0 1 2 3 4 5 6 7 8 9
0 1 2 3 4 5 6 7 8 9
KSL Cells
B
Percentage PSR staining area
***
Control
KSL
B
Control
KSL
C
mg Hydroxyproline / g Liver
*
Control
KSL
D
Control
KSL
Percentage αSMA area
***
Control
KSL
E
αSMA fold change
***
Control
KSL
col1a1 fold change
***
Control
KSL
F
Albumin g/dl
**
Control
KSL
G
Percentage area panCK positive
**
Control
KSL
Control
KSL

Figure 3

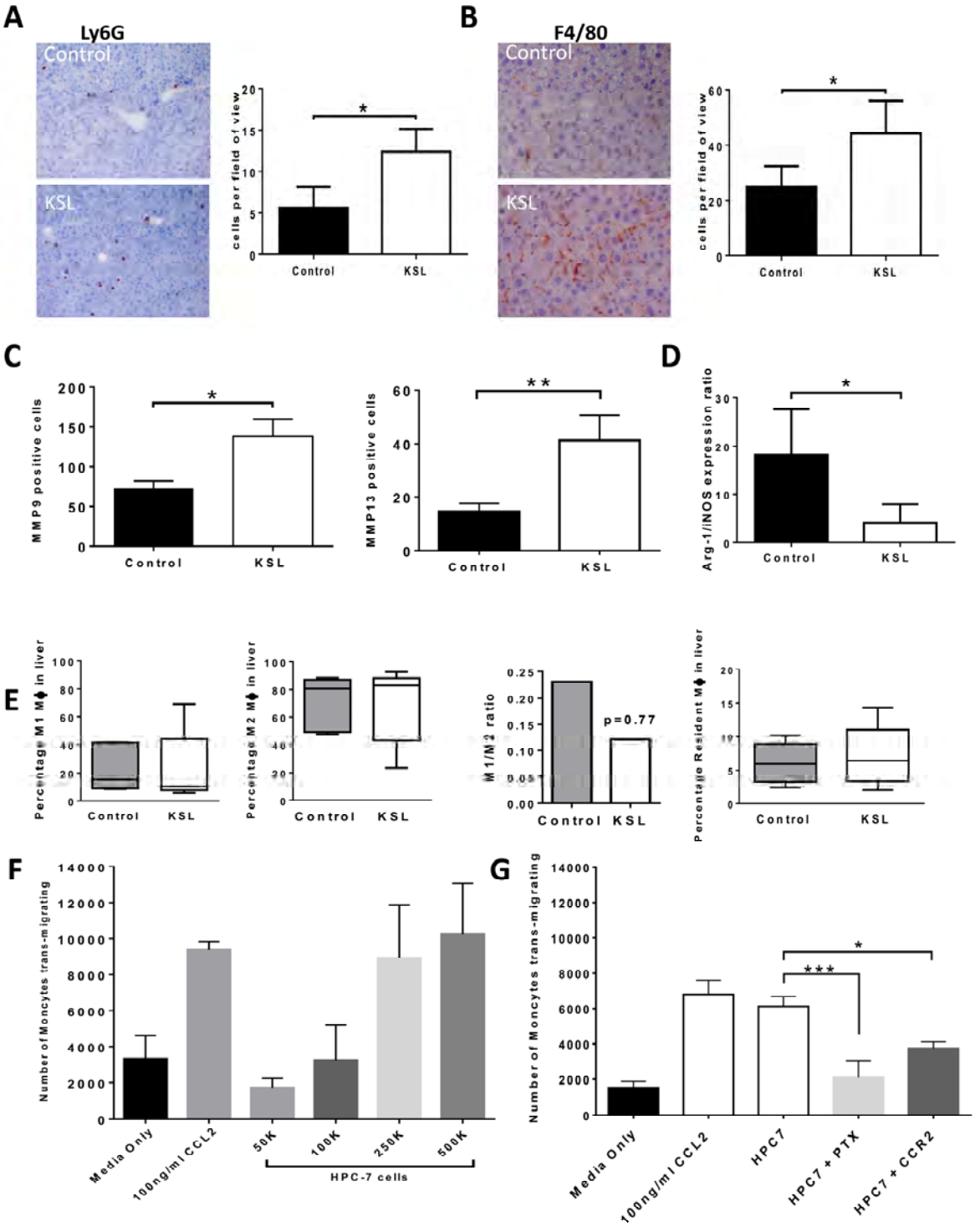
A
Ly6G
Control
KSL
cells per field of view
Control
KSL
B
F4/80
Control
KSL
cells per field of view
Control
KSL
C
MMP9 positive cells
Control
KSL
MMP13 positive cells
Control
KSL
D
Arg-1/iNOS expression ratio
Control
KSL
E
Percentage M1 MΦ in liver
Control
KSL
Percentage M2 MΦ in liver
Control
KSL
M1/M2 ratio
p=0.77
Control
KSL
Percentage Resident MΦ in liver
Control
KSL
F
Number of Moncytes trans-migrating
Media Only
100ng/ml CCL2
50K
100K
250K
500K
HPC-7 cells
G
Number of Moncytes trans-migrating
Media Only
100ng/ml CCL2
HPC7
HPC7 + PTX
HPC7 + CCR2

Figure 4

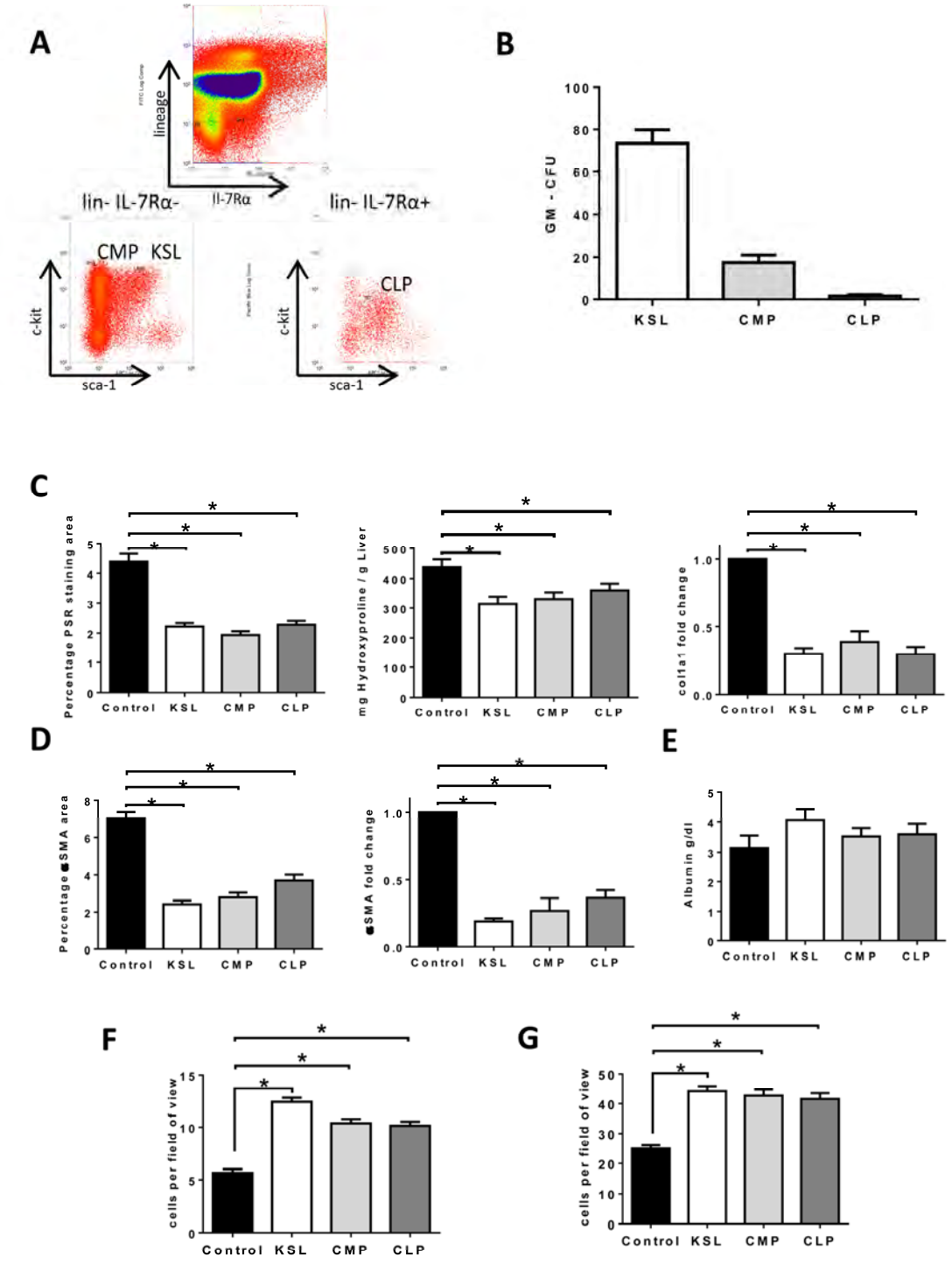
A
lineage
IL-7Rα
lin- IL-7Rα-
lin- IL-7Rα+
CMP KSL
CLP
c-kit
sca-1
B
GM - CFU
KSL
CMP
CLP
C
Percentage PSR staining area
mg Hydroxyproline / g Liver
col1a1 fold change
Control KSL CMP CLP
D
Percentage αSMA area
αSMA fold change
E
Albumin g/dl
F
cells per field of view
G
cells per field of view

Figure 5

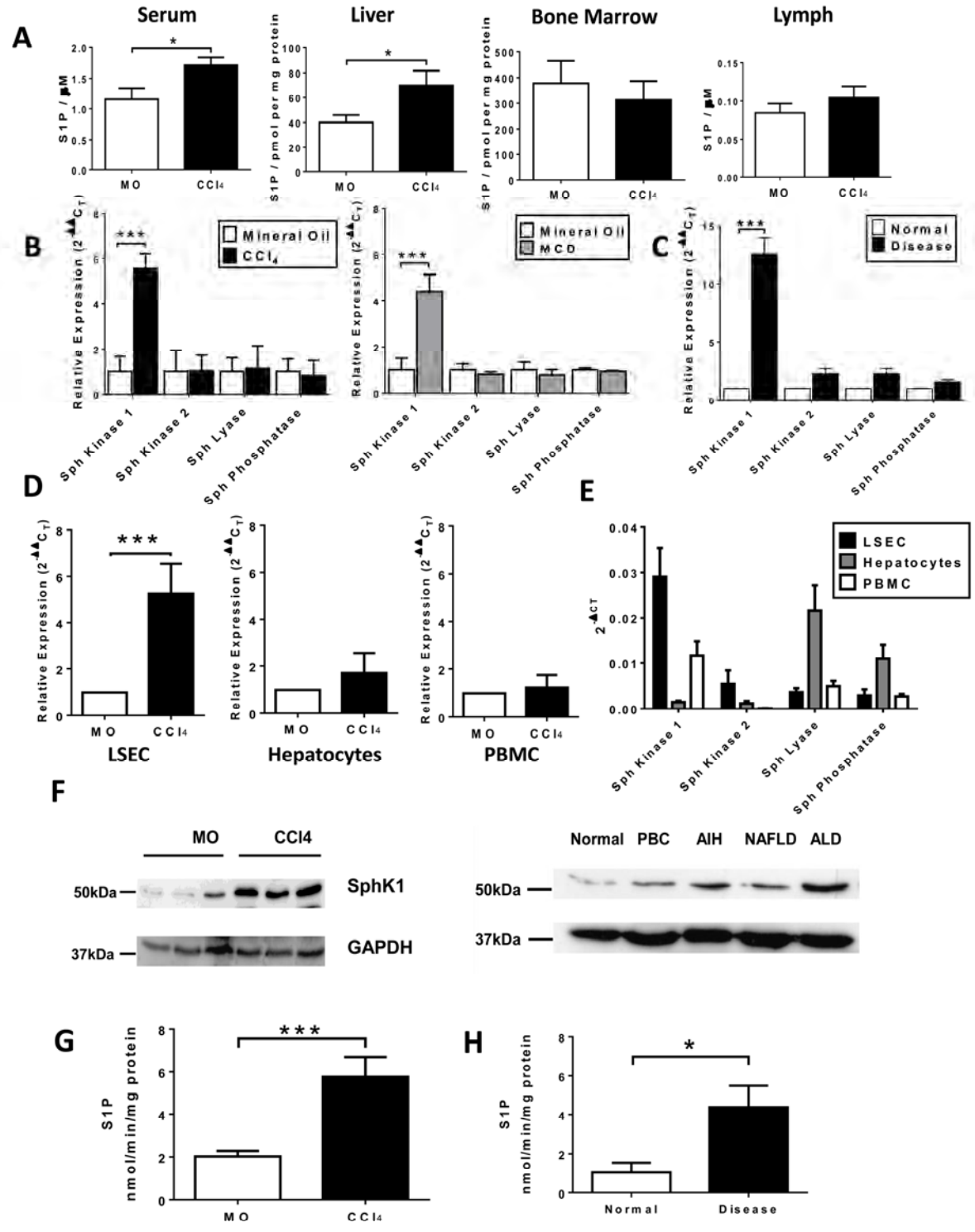
A
Serum
Liver
Bone Marrow
Lymph
S1P / μM
S1P / pmol per mg protein
MO
CCl4
B
Mineral Oil
CCl4
MCD
Relative Expression
Sph Kinase 1
Sph Kinase 2
Sph Lyase
Sph Phosphatase
C
Normal
Disease
D
LSEC
Hepatocytes
PBMC
E
F
MO
CCl4
50kDa
37kDa
SphK1
GAPDH
Normal
PBC
AIH
NAFLD
ALD
G
S1P
nmol/min/mg protein
H

Figure 6

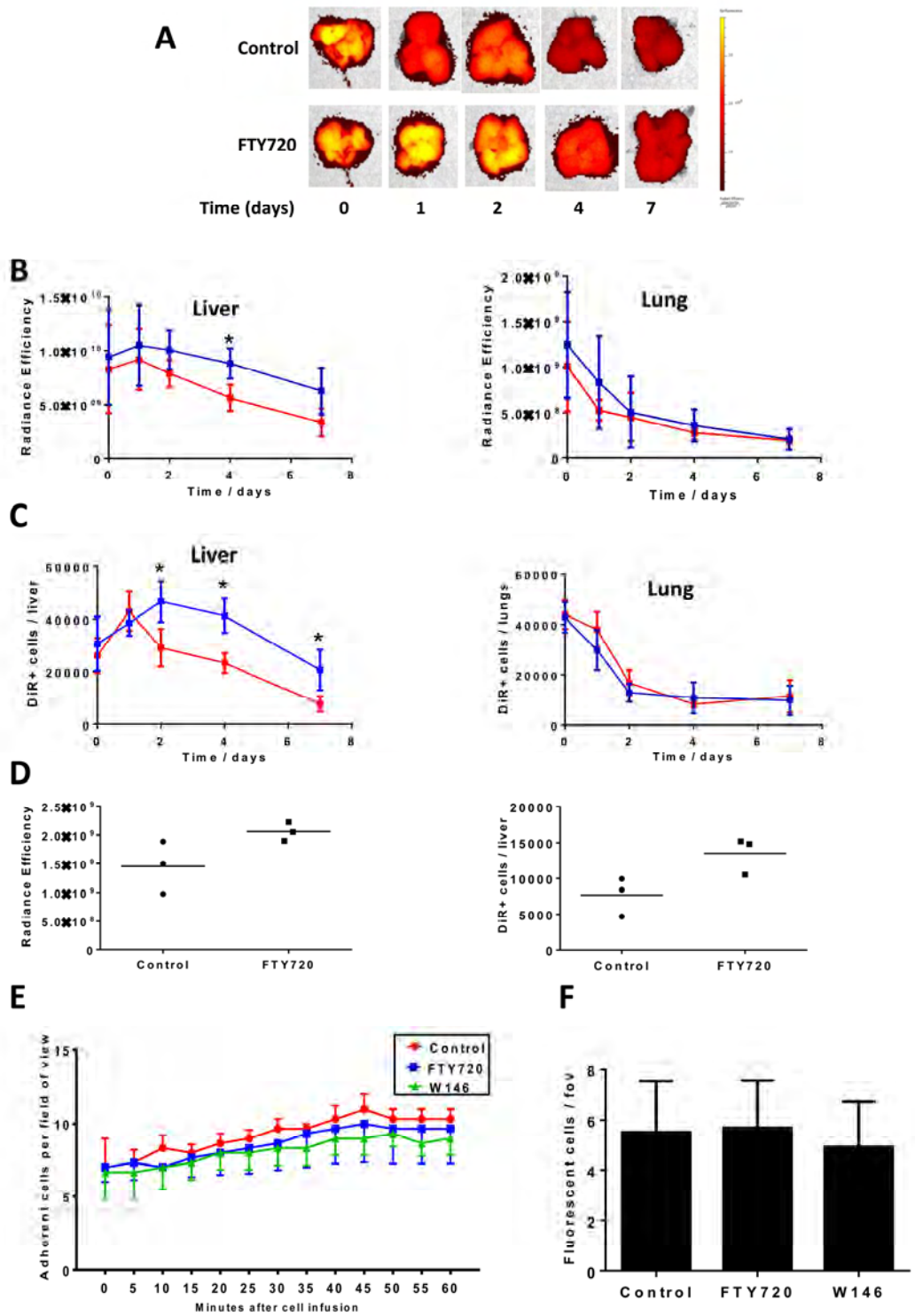
A
Control
FTY720
Time (days)
0
1
2
4
7
B
Liver
Lung
Radiance Efficiency
Time / days
C
Liver
Lung
DiR+ cells / liver
DiR+ cells / lungs
Time / days
D
Radiance Efficiency
DiR+ cells / liver
Control
FTY720
E
Adherent cells per field of view
Control
FTY720
W146
Minutes after cell infusion
F
Fluorescent cells / fov
Control
FTY720
W146

Figure 7

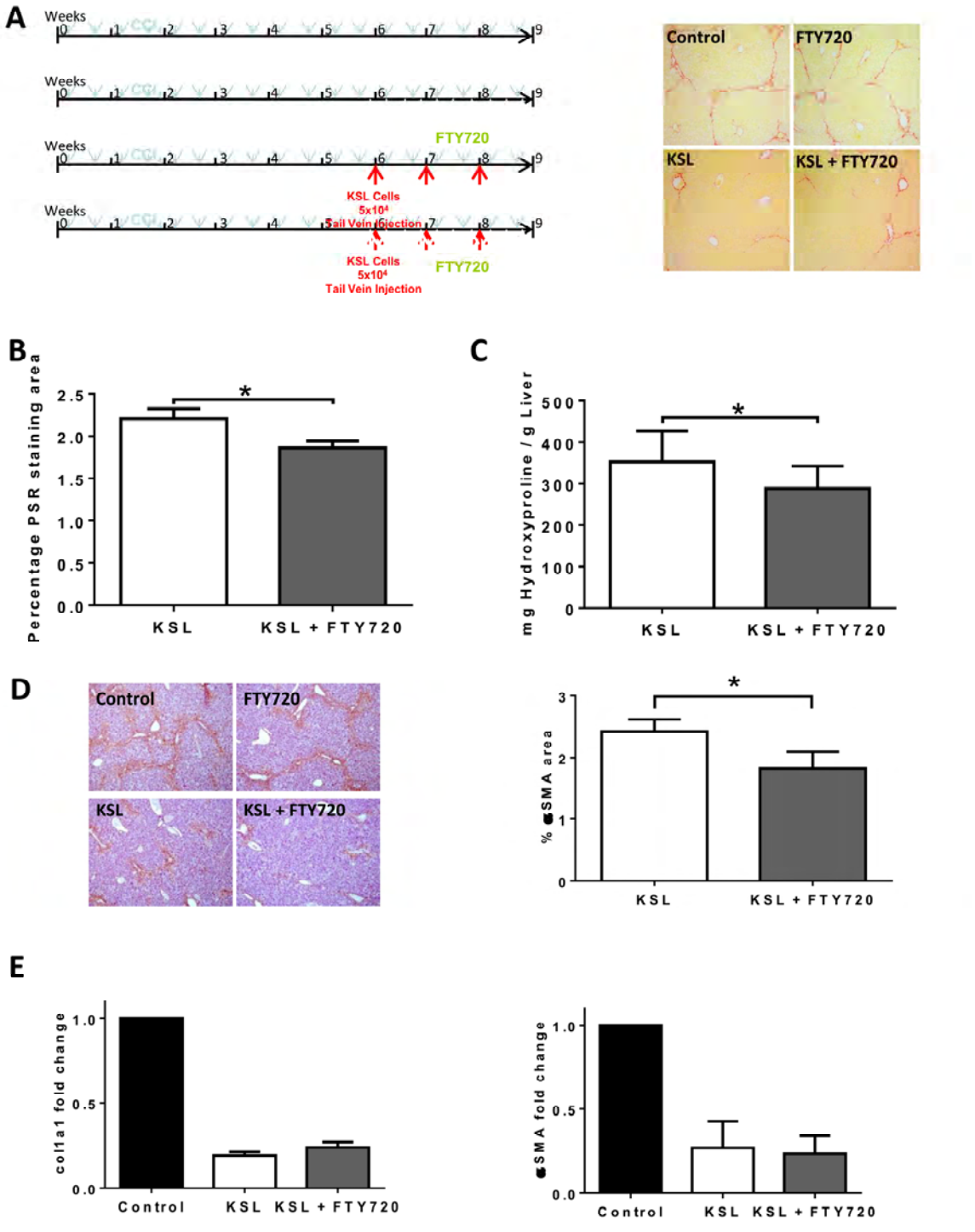
A
Weeks
FTY720
KSL Cells
5x10⁴
Tail Vein Injection
KSL Cells
5x10⁴
Tail Vein Injection
FTY720
Control
FTY720
KSL
KSL + FTY720
B
Percentage PSR staining area
KSL
KSL + FTY720
C
mg Hydroxyproline / g Liver
KSL
KSL + FTY720
D
Control
FTY720
KSL
KSL + FTY720
% αSMA area
KSL
KSL + FTY720
E
col1a1 fold change
Control
KSL
KSL + FTY720
αSMA fold change
Control
KSL
KSL + FTY720

Supplementary material

Methods

Tissue Preparation

Blood samples were obtained by cardiac puncture under general anaesthesia and mice were killed by cervical dislocation. Bone marrow cells were flushed from the medullary cavities of the femur and tibia with DMEM + 10% FCS using a 25G needle. A single cell suspension was prepared by passing the cells through a 40um filter (BD Falcon) and analysed by flow cytometry or used for cell sorting. Mouse tissues were harvested and perfused with PBS, dissociated and digested with 2mg/ml collagenase IV (Sigma). Mononuclear cells were isolated by density centrifugation using an Optiprep (Sigma) gradient and the resulting cell suspension used for flow cytometry. Samples of frozen human liver tissue were obtained from patients of the University Hospital Birmingham with chronic liver disease undergoing liver transplantation or from normal organ donor liver not used for transplantation with written informed consent and local ethics committee approval.

Immunohistochemistry

Liver specimens were fixed in 4% paraformaldehyde, embedded in paraffin and cut into 4µm sections. Slides were deparaffinised and antigen retrieval performed using a citrate buffer pH6.0. Primary antibody was added for 1 hour: anti-αSMA (1:400, Abcam), anti-F4/80 (1:200, AbD Serotec), anti-Ly6G (1:500, AbD Serotec), anti-CD45.2 (1:200, eBioscience) followed by secondary antibody (ImmPRESSS Peroxidase anti-rabbit IgG or anti-rat (mouse adsorbed) IgG, Vector Labs) and expression was visualised using ImmPACT DAB reagent (Vector Labs). Sections were counterstained with haematoxylin and mounted using DPX (Fisher Scientific).

Hydroxyproline Assay

Frozen liver tissue samples were weighed and protein precipitated by the addition of 1:1 Trichloroacetic Acid:Water and incubated on ice for 30 minutes. Samples were hydrolysed with 6N HCl in sealed borosilicate tubes and incubated at 120^{o}C for 16 hours and at 80^{o}C until completely desiccated. The precipitate was resuspended in water and filtered. Chloramine T solution was added at room temperature for 20 minutes followed by addition of Ehrlich's solution and incubation at 65^{o}C in a water bath for 15 minutes. After cooling to room temperature, fluorescence readings at 561nm were taken from samples and standards, and hydroxyproline content expressed as mcg per gram liver tissue.

Flow Cytometry and Cell Sorting

Erythrocytes were lysed using ACK red cell lysis buffer (Sigma). After incubation with anti-CD16/32 antibody (1:20, eBioscience) to eliminate non-specific Fc receptor binding, cell suspensions were labelled with the relevant primary antibodies (all 1:100): anti-CD11b-FITC (M1/70), anti-CD5-FITC (53-7.3), anti-CD8a-FITC (53-6.7), anti-Ter119-FITC (TER119), anti-CD45R-FITC (RA3-6B2), anti-Gr1-FITC (RB6-8C5), anti-CD117(c-kit)-PE, anti-CD117(c-kit)-Pacific Blue, anti-CD117(c-kit)-APC-Cy7 (all 2B8), anti-Sca1-APC (D7), anti-CD127(IL-7Ra)-PE (A7R34), anti-EDG1(S1P1)-PE (T4-H28), anti-CD45.1-PE (A20), anti-CD45.2-APC (104) and incubated on ice for 30 minutes. Non-viable cells were excluded using LIVE/DEAD stain (Invitrogen). Absolute cell counts were determined using Trucount beads (Invitrogen) and data analysed using a CyAn ADP flow cytometer with Summit 4.3 software. Cell sorting was performed using a MoFloCell Sorter (Dako) with Summit 5.2 software. Cells to be injected were sorted directly into sterile PBS and used immediately, whilst cells for PCR analysis were sorted directly into RLT lysis buffer ready for RNA extraction.

Cell isolation from blood and liver and flow cytometric analysis

Blood was collected through cardiac puncture into EDTA tubes. Red blood cells were lysed with 5min lysis buffer. Isolated cells were then washed twice and resuspended in MACS buffer (2% FCS and 1mM EDTA). Liver homogenate was filtered after being homogenised with 5ml syringe plunger. Single cells were then overlaid on density gradient of Opti-prep and centrifuged at 1000g for 25min at room temperature. After two washed isolated cells were then suspended in MACS buffer.

Antibodies used for flow cytometry are listed in table below. Single-cells suspensions were blocked with anti-mouse FcR antibody (CD16/CD32) for 15min at 4C in MACS buffer, and stained with primary conjugated antibodies. For internal staining, cells were fixed and permeabilized with a Foxp3/Permeabilization kit (eBiosciences). Flow cytometry was performed with Fortessa (BD Biosciences) with forward-and side-scatter gates set to exclude non-viable cells. Data were analysed with Flowjo software (version 10.1).

Antibodies	Clone	Conjugate	Source
live/dead		APC-CY7 e780	Life Technology
CD45.2	104	eFluor 506	Ebio
Foxp3	FJK-16s	APC	Ebio
CD3	17A2	eFluor 450	Ebio
CD4	GK1.5	FITC	Ebio

NkP46	29A1.4	PE	Ebio
CD8	53-6.7	BV 786	Biolegend
LY6C	HK1.4	PE	Ebio
LY-6G / Gr-1	1A8-Ly6g	APC	Ebio
CD3	17A2	BV650	Biolegend
B220	Ra3-6B2	eFluor 450	Ebio
CD11b	M1/70	PE-e610	Ebio
F4/80	BM8	PE-CY7	Ebio
CD45.2	104	FITC	Ebio
CD16	93	purified	Ebio

Flow cytometric analysis showing liver macrophages (gated $CD45^{+}CD3^{-}CD11b^{+}F4/80^{+}Ly\text{-}6G^{-}$), resident (res) macrophages (gated $CD45^{+}CD3^{-}CD11b^{int}F4/80^{+}$), M1-macrophages (gated $CD45^{+}CD3^{-}CD11b^{+}F4/80^{+}Ly\text{-}6G^{-}Ly6C^{hi}$), M2-macrophages (gated $CD45^{+}CD3^{-}CD11b^{+}F4/80^{+}Ly\text{-}6G^{-}Ly6\text{-}C^{lo}$)

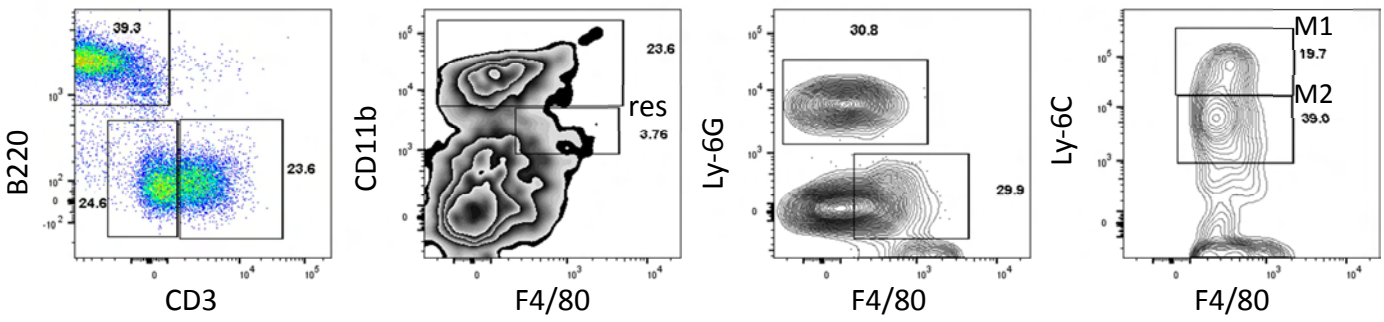

qRT-PCR

RNA extraction was performed using the RNeasy Mini (liver tissue) and Micro (isolated cells) kits (Qiagen) according to manufacturer's instruction, concentration and purity were checked using a Nanodrop 1000 (Thermo Scientific). cDNA was transcribed from RNA using iScript reverse transcriptase (Bio Rad) . RT-PCR was performed on an ABI Prism 7900HT or Stratagene MX3000p using Taqman assay mix pre-designed Taqman assays as detailed in supplementary information (Applied Biosystems). The programme consisted of activation at 95^{o}C for 10 minutes followed by 40 cycles of denaturing (95^{o}C 10 seconds) and annealing (60^{o}C 60 seconds) with fluorescence detection at the end of each cycle. Normalisation to GAPDH using the $2^{-\Delta\Delta CT}$ method was performed and expression relative to the appropriate control calculated.

Serum Albumin

Serum albumin concentrations were determined using the Quantichrom BCG Albumin Assay (Bioassay Systems) according to manufacturer's instructions.

Western Blotting

Whole liver protein extracts were quantified using Bradford reagent and 50µg used for Western blotting. Primary antibody was either anti-SphK1 (1:500, Abcam) or anti-GAPDH (1:2000, Sigma) incubated overnight and HRP conjugated goat anti-rabbit IgG antibody (1:10000, Sigma) secondary antibody incubated for 30 minutes. Pierce chemiluminescent peroxidase substrate and Hyperfilm ECL were used to visualise protein expression.

Transwell migration

Male C57/BL6 mice were culled by cervical dislocation and their tibias and femurs were dissected from the cadavers for monocyte isolation. Ends of bones were trimmed and the bone marrow was flushed out with MACs buffer (PBS+2mM EDTA+0.5%BSA). Following centrifugation and cell count, monocytes were selected from the cell suspension using magnetic labelling and separation. After washing, the cells were resuspended in MACs buffer and incubated for five minutes at 4^{o}C with FcR Blocking Reagent and Monocyte Biotin-Antibody cocktail. The cells were then washed before being incubated with Anti-Biotin Microbeads for ten minutes at 4^{o}C and then passed through an LS column. The unlabelled cells represented the monocyte population and passed through the column. Monocytes were then incubated with cell tracker green for 20 minutes at room temperature (the cell tracker green is diluted 1:1000 to give a concentration of 5µM). CCL2 was prepared in migration media (RMPI+1% PSG+0.1%BSA) to a concentration of 100ng/ml, and 150µl of this added to the receiver plate along with media alone, unstained monocytes and HPC-7 cells. Monocytes were washed and resuspended in migration media to generate a density of 2x10^{5} cells/50µl. 50µl of stained monocytes were then added to the transwell insert and the plate is incubated for four hours at 37^{o}C. After this incubation, samples were collected from the receiver plate and placed into separate FACS tubes. Cells were then washed, resuspended in MACs buffer and quantified flow cytometrically.

Near infra-red fluorescence imaging

1,1'-dioctadecyltetramethyl indotricarbocyanine iodide (DiR, Invitrogen) was dissolved in methanol (1mg/ml) and stored in the dark. 5µl/ml of DiR stock solution was added to cells at 1x10^{6}/ml in complete StemPro media and incubated in the dark for 30 minutes at 37^{o}C. Cells were washed and resuspended in 100-200µl sterile PBS for reinjection.

Near infra-red imaging was performed using the IVIS Spectrum Imaging System (auto exposure, medium binning, excitation wavelength 745nm, emission wavelength 800nm). Fluorescence of individual organs was determined by Living Image Software (Perkin Elmer) using region of interest (ROI) analysis after subtraction of background and expressed by as radiance efficiency (calculated as: radiance of subject / illumination intensity) to eliminate variability in the excitation light across the field of view.

Intravital Microscopy

C57BL6 mice with 8 weeks of CCl_4 liver injury underwent ketamine/xylazine anaesthesia and carotid artery cannulation. Laparotomy was performed and the liver was exteriorised and placed on the stage of an Olympus IX81 inverted microscope. One x10 power field of view was selected for imaging. HPC-7 cells were labelled with 5µM CFSE and injected, one minute video recordings of the selected field of view were taken every 5 minutes until 60 minutes and analysed for adhesion (stationary >30 seconds) of labelled cells using Slidebook software (Intelligent Imaging Innovations).

Supplementary Figure 1. Bone marrow transplantation studies

(A) Recipient BoyJ (CD45.1) mice received Baytril antibiotic in drinking water one week prior and one week following irradiation with 9Gy in two divided doses on the same day. Bone marrow cells were obtained from donor C57BL6 (CD45.2) mice by flushing of the tibia and femurs. Six hours following irradiation donor bone marrow cells were infused into recipient mice by tail vein injection. After 4 weeks recovery, transplanted mice were divided into two groups at random with one group receiving twice weekly intraperitoneal administration of carbon tetrachloride (1mg/kg) in mineral oil and the other group receiving intraperitoneal injections of mineral oil alone for a further 8 weeks. (B,C) Samples of bone marrow and peripheral blood were treated with red cell lysis buffer and

labelled with fluorescent antibodies to CD45.1 and CD45.2. Analysis of CD45 expression by flow cytometry revealed almost complete CD45.2 expression following transplantation compared with CD45.1 expression prior to transplantation. Representative flow cytometry plots of multiple experiments are shown.

Supplementary Figure 2. Isolation of KSL cells

Bone marrow cells were obtained from donor mice following dissection of the tibia and femurs by flushing the marrow cavity with DMEM + 10%FCS. Cells were treated with red cell lysis buffer and filtered prior to labelling with fluorescently conjugated antibodies to lineage specific markers (CD11b, CD8a, CD5, Ter119, Gr-1, B220), c-kit and sca-1. Cells were isolated by initially excluding dead cells and debris on a forward scatter – side scatter plot (A) and excluding doublets of cells on a forward scatter – pulse width plot (B). The lineage negative population was determined (C) and plotted according to expression of c-kit and sca-1 surface markers (D). HSC were defined as c-kit+, sca-1+ and lineage marker negative ('KSL') and represented 0.05% of the total bone marrow cell population. The purity of the isolated cells was then checked by determining lineage marker, c-kit and sca-1 expression on a sample of isolated cells (E).

Supplementary Figure 3. Impact of administered haematopoietic stem cells (HSC) on endogenous peripheral blood monocytes.

Flow cytometric analysis of peripheral blood was undertaken to characterise the macrophage sub-sets (M1/M2) and their ratio (C). The following gating strategy was utilised: M1-macrophages (gated $CD45^{+}CD3^{-}CD11b^{+}F4/80^{+}Ly\text{-}6G^{-}Ly6C^{hi}$) and M2-macrophages (gated $CD45^{+}CD3^{-}CD11b^{+}F4/80^{+}Ly\text{-}6G^{-}Ly6\text{-}C^{lo}$). Data are expressed as median +/- IQR.

Supplementary Figure 4. S1P gene expression in extra-hepatic organs

Chronic liver injury was induced in age and sex matched C57/BL6 mice by twice weekly intraperitoneal administration of carbon tetrachloride (1mg/kg) in mineral oil for 8 weeks. Control mice received twice weekly intraperitoneal injections of mineral oil. Mice were sacrificed and gene expression of sphingosine kinase 1, sphingosine kinase 2, sphingosine lyase and sphingosine phosphatase relative to GAPDH was determined in (A)spleen, (B) kidney and (C) lung. Bars represent mean +/- SEM fold change relative to control mice. N=5 per group.

Supplementary Figure 5. Hepatic gene expression across differing aetiologies of liver disease

Samples of frozen liver tissue were obtained from either normal donor liver or explanted livers from patients with liver disease (ALD Alcoholic liver disease, PBC primary biliary cirrhosis, AIH Autoimmune hepatitis, NAFLD Non-alcoholic fatty liver disease, HCV Hepatitis C virus, POD Paracetamol overdose). Gene expression of sphingosine kinase 1, sphingosine kinase 2, sphingosine lyase and sphingosine phosphatase relative to GAPDH was determined. Bars represent mean +/- SEM fold change relative to normal liver (no statistical comparison, n=3 per group).

Supplementary Figure 6. Characterisation of HPC-7 cell line

(A) Cultured HPC-7 cells were labelled with fluorescently conjugated antibodies to lineage markers (CD11b, CD5, CD8a, Ter119, Gr-1, B220), c-kit and sca-1 and analysed by flow cytometry. Dead cells and debris were excluded by gating on a plot of forward scatter – side scatter and surface expression of lineage markers, c-kit and sca-1 measured. Representative histograms displayed (isotype control: grey, antibody: red line). (B) HPC-7 cells were cultured in Methocult GF media for 7 days and significant numbers of myeloid colony forming cell clusters were identified. Representative image of

CFU-GM colony shown. (C) Gene expression of S1P receptors 1-5 in cultured HPC-7 cells relative to GAPDH by the $2^{-\Delta CT}$ method was determined. Bars represent mean +/- SEM expression in three independent experiments. (D) Surface S1P1 receptor expression on cultured HPC-7 cells was analysed by flow cytometry. After fixation and permeabilisation of the cells, total intracellular S1P1 receptor expression was also assessed. Representative histograms of 3 independent experiments are displayed (grey area: isotype control, red line: S1P1 antibody). (E) $1x10^6$ HPC-7 cells were added to the top well of the transwell and migration to varying concentrations of S1P proceeded for 4 hours. Cells migrating into the bottom well were counted using flow cytometry and expressed as a percentage of the total number of HPC-7 cells added to the top well. Bars represent the mean +/- SEM of 3 separate experiments.

Supplementary Figure 7. Chemokine receptor expression on KSL and HPC-7 cells

Gene expression of chemokine receptors in (A) freshly isolated KSL cells and (B) cultured HPC-7 cells was determined by quantitative PCR. Expression relative to GAPDH by the $2^{-\Delta CT}$ method was determined. Bars represent mean +/- SEM expression in three independent experiments.

Supplementary Figure 8. FTY720 alters HSC trafficking through modulation of S1P1

(A) Gene expression of S1P receptors 1-5 was determined in freshly isolated KSL cells relative to GAPDH by the $2^{-\Delta CT}$ method. Bars represent mean +/- SEM expression in three independent experiments. (B) Surface and total S1P1 receptor expression on freshly isolated KSL cells was analysed by flow cytometry. Representative histograms of three independent experiments are displayed (grey area: isotype control, red line: S1P1 antibody). (C) $1x10^5$ KSL cells were added to the top well of a transwell and migration to varying concentrations of S1P assessed over a 4 hour period. Cells migrating into the bottom well were analysed for expression of c-kit and sca-1 and quantified

by flow cytometry. KSL cells migrating to the lower well were expressed as a percentage of the total number of KSL cells added to the top well. Bars represent the mean +/- SEM of three separate experiments. (D) S1P receptor dependence of migration of KSL cells to S1P was assessed by placing cells in the upper-chamber of a trans-well and quantifying their migration to the presence or absence of S1P in the lower chamber. Treatment of KSL cells with either FTY720 (S1P receptor partial agonist) or W146 (S1P receptor 1 antagonist) inhibited their migration to S1P in trans-well assays (three independent experiments). (E) Administration of daily intraperitoneal FTY720 (1mg/kg) for seven days in CCl_4 injured mice resulted in an increased number of KSL cells in the liver but circulating KSL cells remained unchanged (n=6 per group, two independent experiments). * $p<0.05$

Supplementary Figure 9. Validation of DiR staining

(A) Fluorescence intensity of varying numbers of cells labelled with 5μM DiR was measured using the IVIS imaging system. n=3, mean+/-SD fluorescence shown. (B) Representative IVIS image (fluorescence intensity overlaid on photograph) of indicated numbers of cells labelled with 5μM DiR at each. Freshly isolated KSL cells were incubated with 5μM DiR for 10 minutes at room temperature, washed and resuspended in media. (C) Cell viability of labelled cells (black bars) was measured by viability dye exclusion determined by flow cytometry and compared with unlabelled cells (white bars). n=3, mean+/-SD % dead cells shown. (D) Colony forming ability in labelled (black bars) and unlabelled (white bars) cells was measured by in vitro methylcellulose assay. n=3, mean +/- number of colonies formed shown. (E) Loss of fluorescence over time: $1x10^6$ cultured HPC-7 cells were labelled with 5μM DiR for 10 minutes at room temperature, washed and resuspended in complete media. A cell sample was taken at each time point and MFI determined by flow cytometry. (F) Potential transfer of dye from labelled to unlabelled cells: $1x10^6$ cultured HPC-7 cells were labelled with 5μM DiR for 10 minutes at room temperature, washed and resuspended in complete media together with $1x10^6$ unlabelled HPC-7 cells. A cell sample was taken at each time point and

the percentage of fluorescent DiR labelled cells in the sample determined by flow cytometry. n=3, mean+/- SD % fluorescently labelled cells shown.

Supplementary Figure 10. Use of FTY alone in model of chronic liver injury

Chronic liver injury was induced in age and sex matched C57/BL6 mice by twice weekly intraperitoneal administration of carbon tetrachloride (1mg/kg) in mineral oil for 6 weeks, mice were then randomly allocated to a treatment group. Mice in the control group continued to receive twice weekly injections of intraperitoneal carbon tetrachloride until week 10 and were sacrificed 72 hours following the final injection of carbon tetrachloride. Mice in the FTY720 treatment group received twice weekly carbon tetrachloride in the same way as control mice but in addition received thrice weekly FTY720 (1mg/kg) via intraperitoneal injection from the start of week 7, mice were sacrificed at the start of week 10, 72 hours after the final injection of carbon tetrachloride. (A)Formalin fixed paraffin embedded liver tissue sections from control mice (black bars) and mice treated with FTY720 (grey bars) were stained for picrosirius red. 6 random, non-overlapping images were obtained from each section and staining was quantified as a percentage of the image positive for picrosirius red using ImageJ software. n=12-13 each group, mean +/-SD % area stained shown, p=ns. (B) Hydroxyproline content in samples of liver tissue from control mice (black bars) and mice treated with FTY720 (grey bars) was determined and expressed as mg of Hydroxyproline per gram of liver tissue. n=12-13 each group, mean+/-SD hydroxyproline content shown, p=ns. RNA was extracted from liver tissue of control mice (black bars) and mice treated with FTY720 (grey bars) and using quantitative RT-PCR gene expression of (C) col1a1 and (E) □SMA were determined, normalised to GAPDH expression and relative to control mice using the 2^{-ddCT} method. n=12-13each group, mean +/-SD fold change shown, p=ns. (D) Formalin fixed paraffin embedded liver tissue sections from control mice (black bars) and mice treated with FTY720 (grey bars) were stained for □SMA. 6 random, non-overlapping images were obtained from each section and staining was quantified as a

percentage of the image positive for CD45 using ImageJ software. n=12-13 each group, mean +/-SD

% area stained shown, p=ns (F)

Supplementary Figure 1

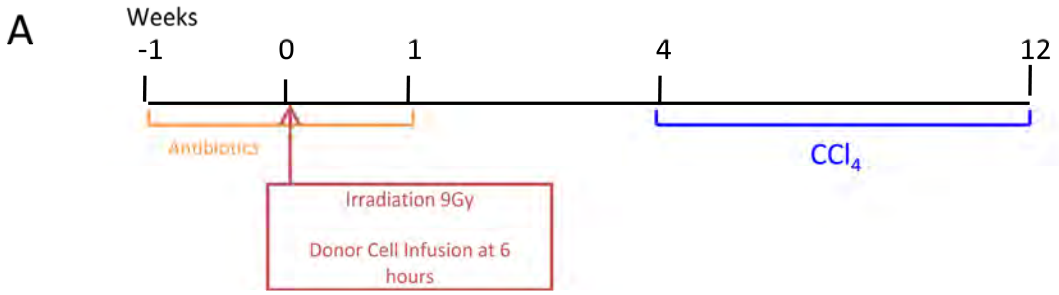

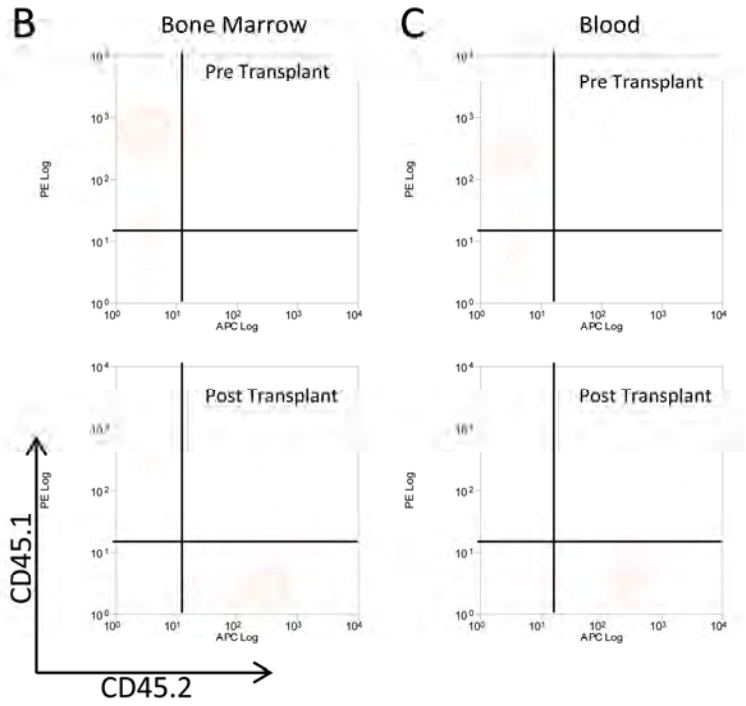

Supplementary Figure 2

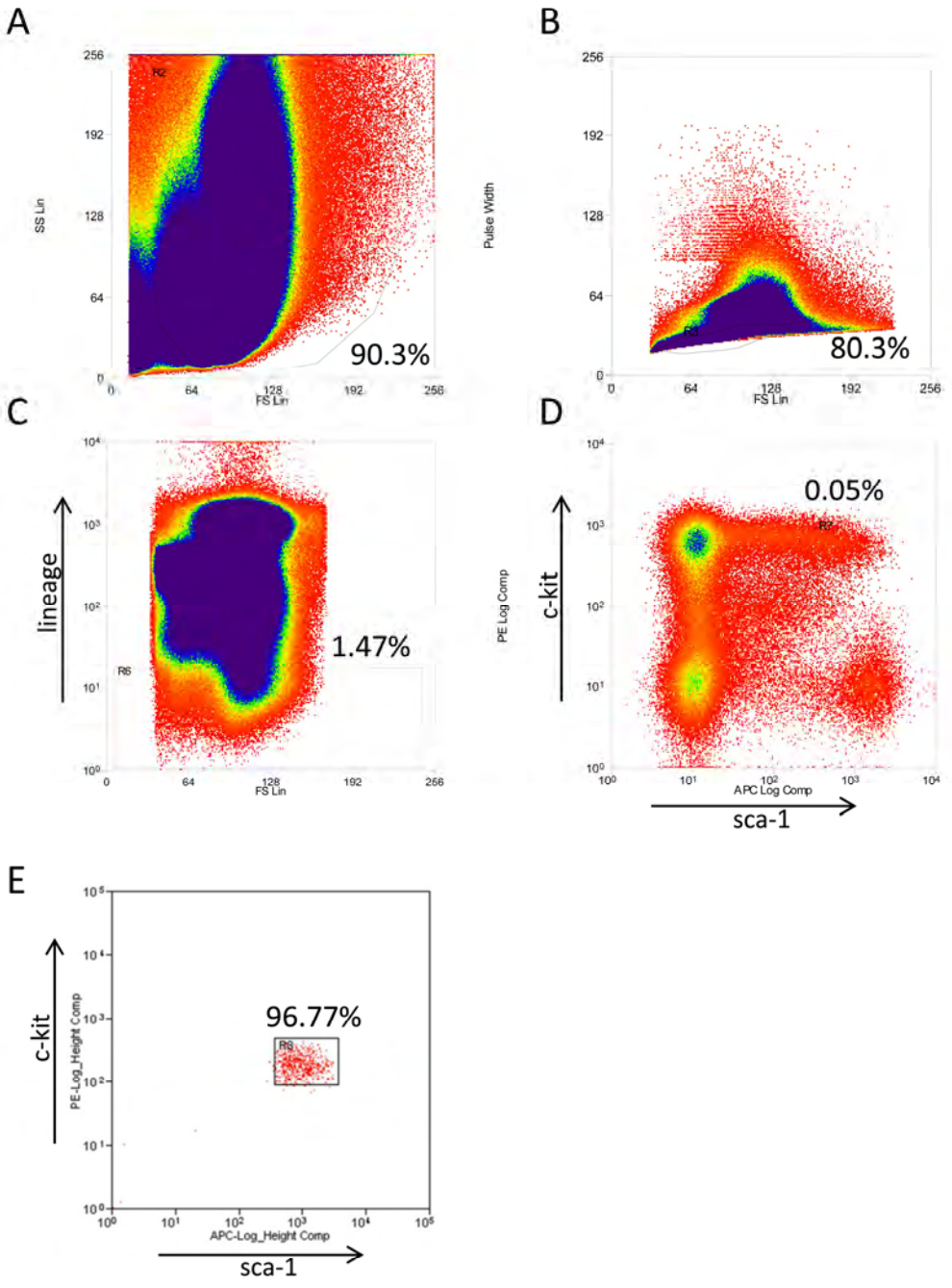

Supplementary Figure 3

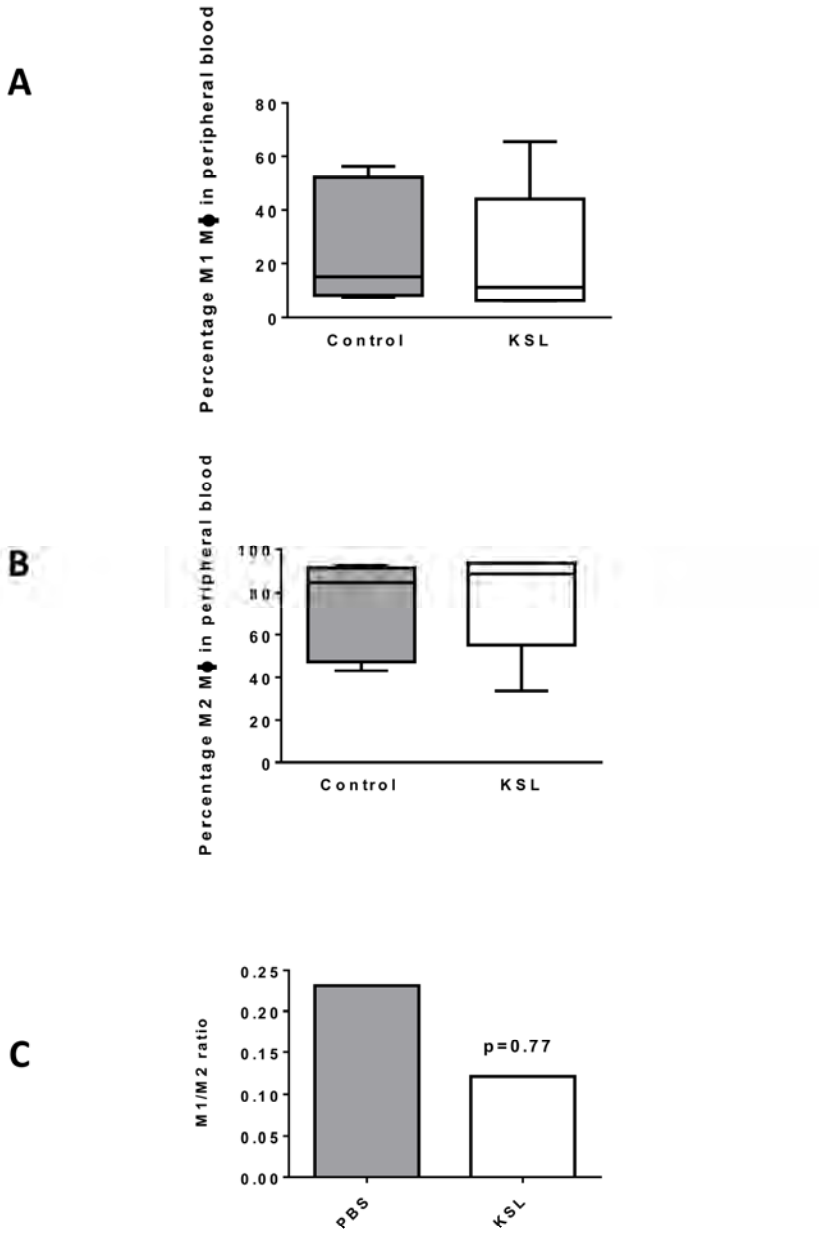

Supplementary Figure 4

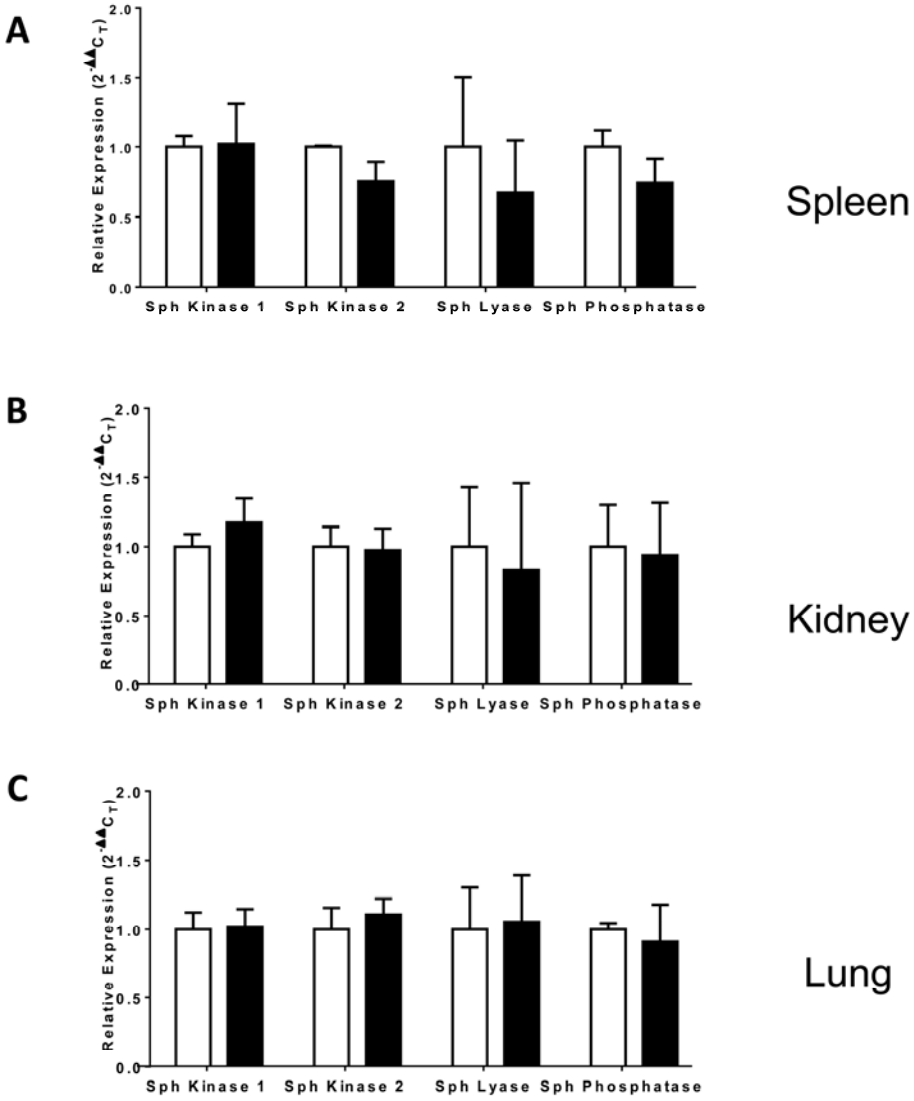

Supplementary Figure 5

A

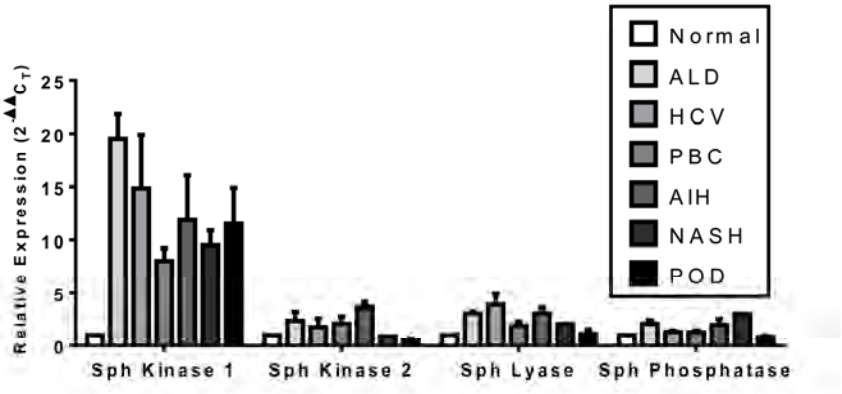

Supplementary Figure 6

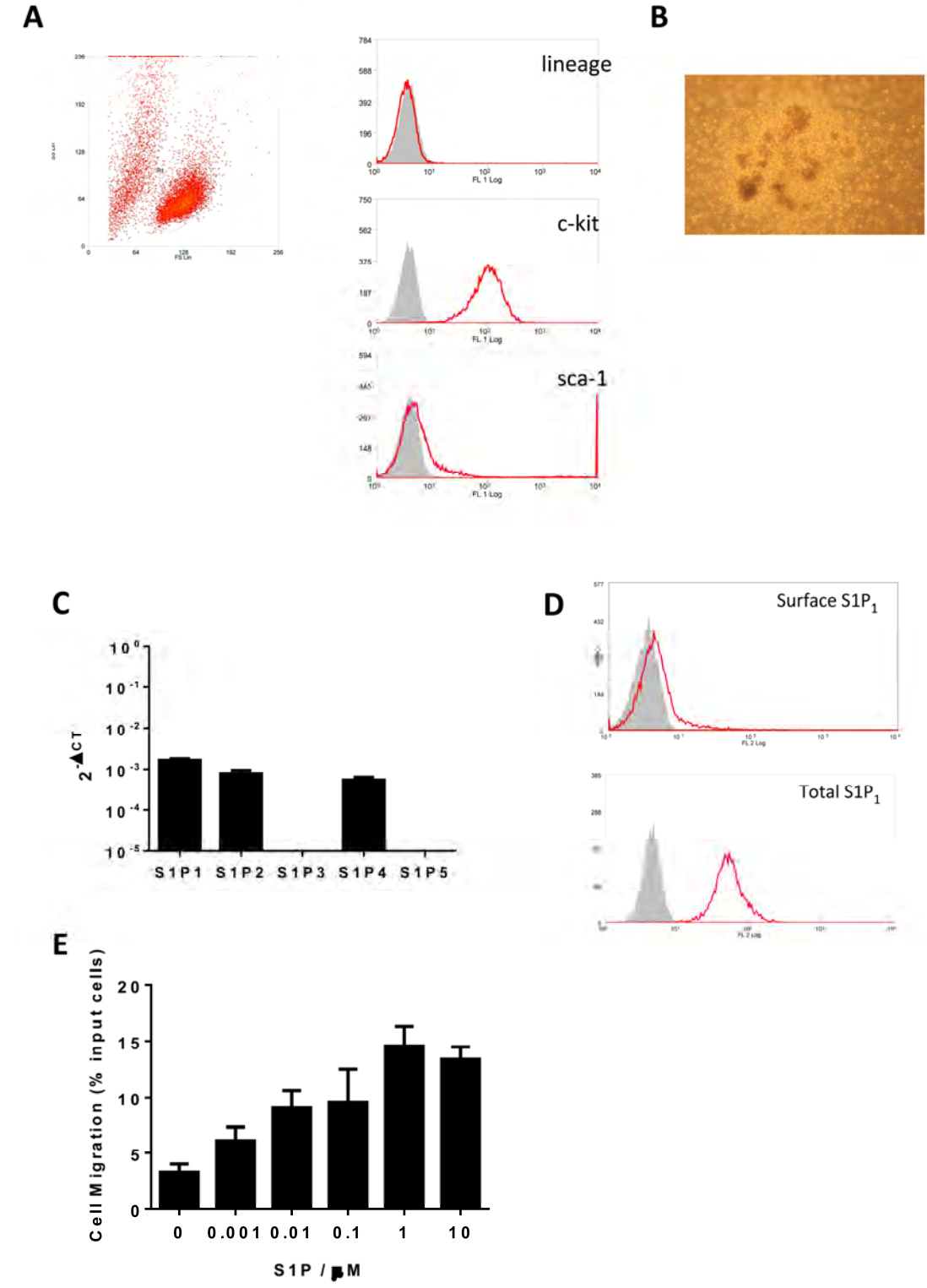

Supplementary Figure 7

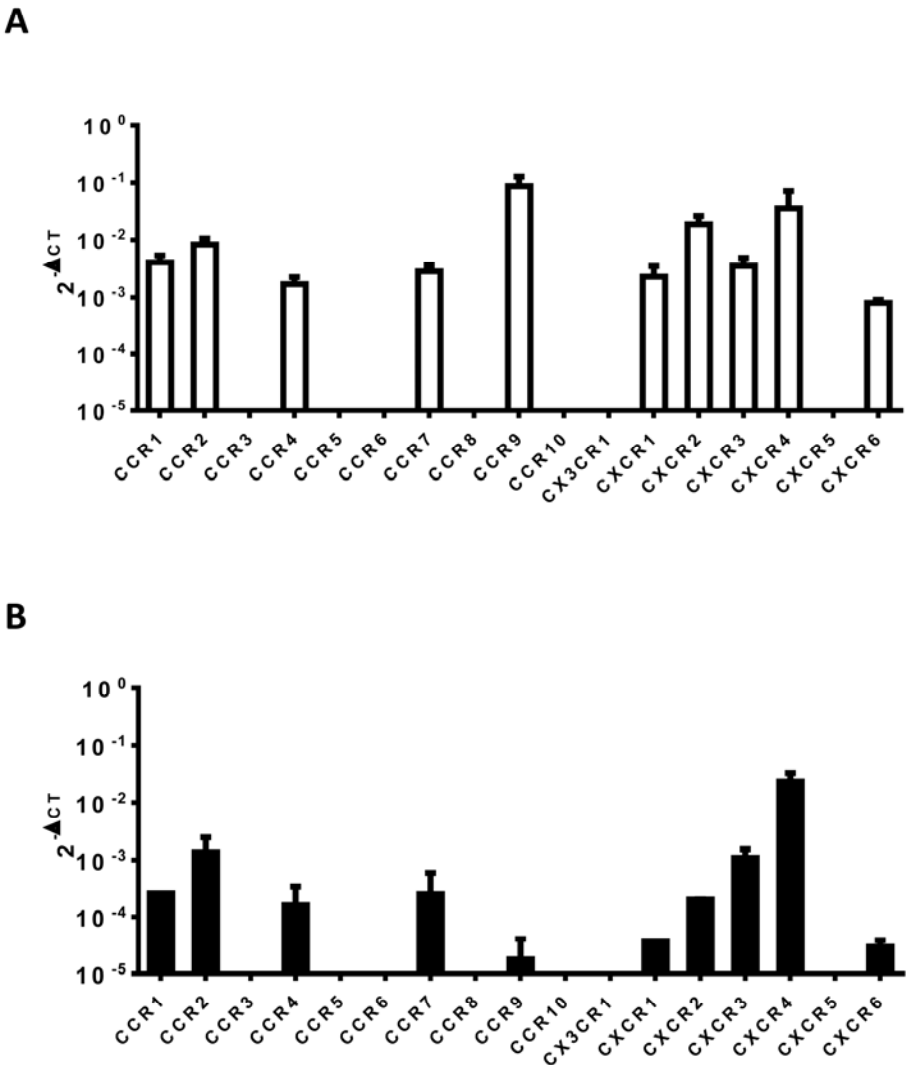

Supplementary Figure 8

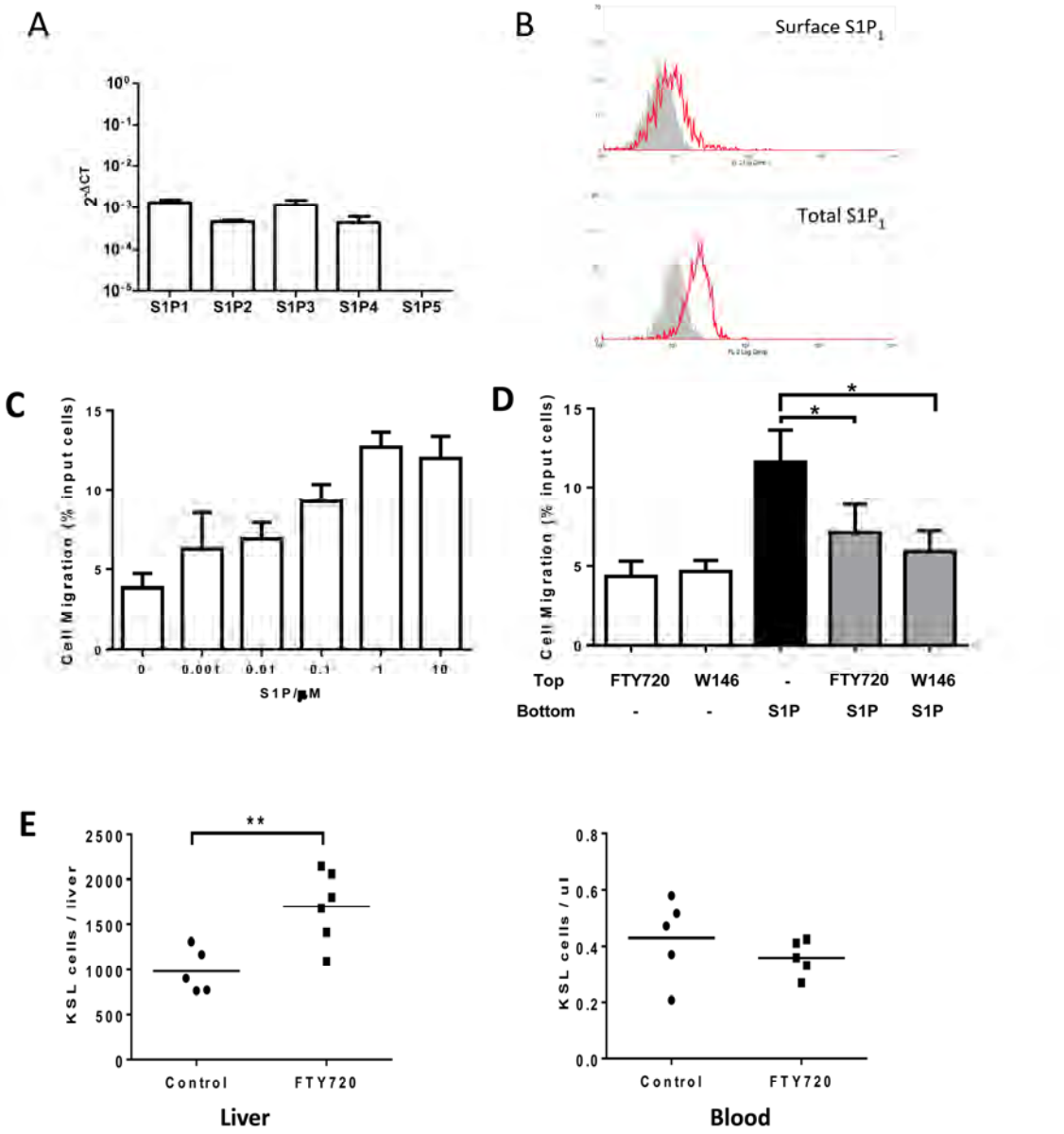

Supplementary Figure 9

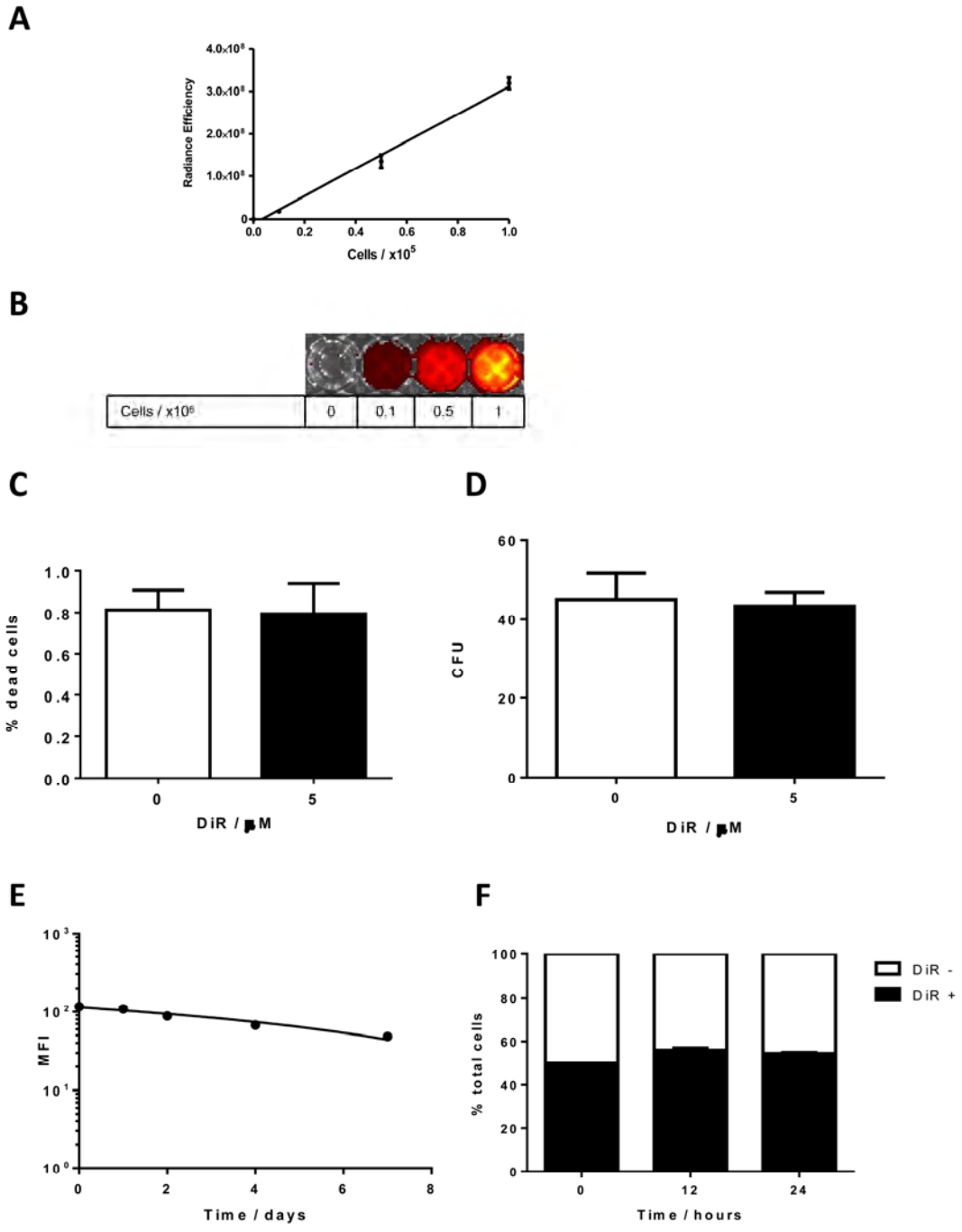

Supplementary Figure 10